

8. SITES 867/868¹

Shipboard Scientific Party²

HOLE 867A

Date occupied: 24 April 1992
Date departed: 25 April 1992
Time on hole: 10 hr 30 min
Position: 21°20.963'N, 174°18.550'E
Bottom felt (rig floor, m; drill-pipe measurement): 1363.2
Distance between rig floor and sea level (m): 11.02
Water depth (drill-pipe measurement from sea level, m): 1352.2
Total depth (rig floor, m): 1373.2
Penetration (m): 10.0
Number of cores (including cores with no recovery): 1
Total length of cored section (m): 10.0
Total core recovered (m): 0.07
Core recovery (%): 0.7
Oldest sediment cored:
Depth (mbsf): 10.0
Nature: Floatstone
Age: Albian

HOLE 867B

Date occupied: 25 April 1992
Date departed: 27 April 1992
Time on hole: 2 days 1 hr 30 min
Position: 21°20.959'N, 174°18.561'E
Bottom felt (rig floor, m; drill-pipe measurement): 1363.2
Distance between rig floor and sea level (m): 11.02
Water depth (drill-pipe measurement from sea level, m): 1352.2
Total depth (rig floor, m): 1440.0
Penetration (m): 76.8
Number of cores (including cores with no recovery): 14
Total length of cored section (m): 76.8
Total core recovered (m): 22.46
Core recovery (%): 29.2
Oldest sediment cored:
Depth (mbsf): 76.8
Nature: Wackestone-packstone
Age: Albian
Measured velocity(km/s): 5.0–6.0

HOLE 868A

Date occupied: 27 April 1992
Date departed: 29 April 1992
Time on hole: 1 day 16 hr
Position: 21°21.171'N, 174°18.564'E
Bottom felt (rig floor, m; drill-pipe measurement): 1396.0
Distance between rig floor and sea level (m): 11.05
Water depth (drill-pipe measurement from sea level, m): 1385.0
Total depth (rig floor, m): 1416.3
Penetration (m): 20.3
Number of cores (including cores with no recovery): 5
Total length of cored section (m): 20.3
Total core recovered (m): 9.40
Core recovery (%): 46.3
Oldest sediment cored:
Depth (mbsf): 20.3
Nature: Floatstone
Age: Albian
Measured velocity (km/s): 6.0–6.5

Principal results: Sites 867/868 (proposed Site Hue-B) are located on the northern rim of the summit of Resolution Guyot in the western Mid-Pacific Mountains. Site 867 (21°20.96'N, 174°18.56'E) is at a depth of 1352 m atop the perimeter mound that fringes the summit of the guyot, whereas Site 868 (21°21.17'N, 174°18.56'E) is on a terrace, approximately 33 m deeper and 400 m outside the perimeter mound. Because of their proximity in space and in scientific theme, the sites have been joined for the purposes of reports. Proposed Site Hue-B was to be a single, shallow-penetration (approximately 300 m) hole drilled into the perimeter mound surrounding the summit of Resolution Guyot. It had been assumed that this mound was a Cretaceous reef that had drowned and perhaps even been emergent owing to relative sea level fall. The goals of drilling at these two sites were as follows:

1. To examine the biota and vertical development of a Cretaceous reef,
2. To determine the cause(s) and timing of drowning, and
3. To determine the magnitude of relative sea level change and its effects.

A second hole (Site 868) was drilled because results from previous Leg 143 sites suggested that a significant gap in time exists between the oldest platform carbonates and the first pelagic sediments to accumulate atop the platform. It was thought that the terrace might be a sea-level lowstand reef complex whose drilling might help to fill the gap. Sites 867/868 are not precisely at the proposed location of Hue-B, but 1.2 and 1.0 nmi (2.2 and 1.9 km), respectively, to the southeast. Because the perimeter mound is lineated along the rim of the summit, we reasoned that almost any location on the mound would produce similar results, so Site 867 was situated at the top of the mound near Site 866. Likewise, Site 868 was occupied by moving 400 m northward to the terrace near Site 867.

Coring began at Site 867 at 2145 UTC, 24 April 1992, and drilling was finished at Site 868 at 1330 UTC, 28 April, after 3.6 days. Two holes were

¹ Sager, W.W., Winterer, E.L., Firth, J.V., et al., 1993. *Proc. ODP, Init. Repts.*, 143: College Station, TX (Ocean Drilling Program).

² Shipboard Scientific Party is as given in list of participants preceding the contents.

drilled at Site 867; both were spudded-in with no guidebase on hard limestone having virtually no sediment cover. The first hole (867A) consisted of a single core drilled with the diamond bit. The small-diameter bottom hole assembly (BHA) sheared off at the outer core barrel, so the hole was terminated. The second hole was drilled with the experimental polycrystalline (PDC) bit, which has cored limestone on land with success. Our thinking was that this bit might improve recovery in the limestones, thus it was pressed into service. The PDC bit cored slowly in hard limestone, but with excellent recovery. Hole 867B was drilled to a depth of 76.9 mbsf in 23.5 hr, with 29.2% average recovery. Average recovery would have been higher, but the section contained a 9-m cavity. Hole 868A, the only hole drilled at that site, penetrated 20.3 mbsf in 16.8 hr and 46.3% of the section was recovered.

Hole 867B was terminated at 76.9 mbsf, rather than the planned 300 mbsf, mainly because at depth the limestone facies reverted to lagoonal, rather than the reefal, facies sought. Consequently, drilling operations were moved downslope to Site 868. Drilling was terminated at Site 868 when time ran out for the drilling schedule; it was necessary to begin transiting to the next site.

Using combined microfossil and macrofossil biostratigraphy, visual core descriptions augmented with smear-slide and thin-section data, physical properties data, and downhole logs, two principal stratigraphic units were recognized (see "Lithostratigraphy" section, this chapter). Cores from Sites 867/868 consist of shallow-water limestone with a thin veneer of pelagic limestone. Based primarily on benthic foraminifers, the shallow-water limestone is Albian in age, whereas planktonic foraminifers and nannofossils indicate Eocene age for the overlying pelagics. Two lithologic units were recognized at Site 867, but Site 868 fit within the second, stratigraphically lower unit from Site 867. The lithologic units are described as follows:

1. Unit II (10.0–0.0 mbsf, Hole 867A; 76.8–0.29 mbsf, Hole 867B; 20.3–0.0 mbsf, Hole 868A). Albian bivalve/gastropod/echinoid wackestone to packstone, grainstone to floatstone beach deposits, and oolitic grainstone. A variable amount of skeletal material is present, including rudists, sponges, and corals. These limestones have two outstanding characteristics. First, they display meter-scale, fining-upward, transgressive-regressive sequences modulating an overall shift from restricted lagoon to open-marine shoreface going up the section. Second, virtually the entire sequence, down to at least 62 mbsf, contains centimeter-scale dissolution cavities, many of which contain speleothems and implying dissolution in the lower vadose zone. Some cavities may be much larger; one section about 9-in length gave no resistance to the drill string and is thought to be a cavity. Unit II has been subdivided into three subunits, the uppermost of which is distinguished by multiple generations of internal sediment (mudstone) of different colors and compositions, the most prominent of which is dark brown, fine-grained phosphatic material. This subunit also gives high readings in the gamma-ray logs, as did the upper limestone layers of Allison Guyot, probably owing to the pervasive phosphatization. The second subunit is essentially the same, except for the absence of cavity infilling and pervasive phosphatization. A notable feature of this subunit is coarse-grained intervals of floatstone to rudstone interbedded with finer-grained wackestone, packstone, and grainstone. The coarser-grained sediments are composed mainly of caprinid rudist and gastropod shell fragments, intraclasts, and peloids. The entire section drilled at Hole 868A has been distinguished as the third subunit because it is characterized by intervals of boundstone that consists of calcic sponge fragments. The boundstone is interbedded with floatstone and grainstone that contains rudists, gastropods, sponge fragments, possible oyster fragments, and oncoidally coated particles. This subunit also contains a layer of red-stained limestone that suggests emergence.

2. Unit I (0.29–0.0 mbsf, Hole 867A). Eocene foraminifer nannofossil limestone, heavily replaced and impregnated with phosphate and manganese dendrites. This unit represents the first permanent pelagic sedimentation at the site.

The facies evolution of Sites 867/868 implies an overall opening of the environment, from restricted lagoon to open-marine foreshore. This trend

is modulated by meter-scale transgressive-regressive cycles. Many of the cycles begin with storm deposits, typically with an erosive base, and grade to lagoon, tidal flat, or beach. The most obvious diagenetic process is dissolution, probably caused by subaerial exposure. Cavities formed by this process in the upper part of the section were partially or wholly filled by a later generation of fine-grained sediment. The final stage of carbonate platform evolution was the deposition of a thin cover of pelagic sediments.

The results from Sites 867/868 have two important implications. First, the dissolved cavities with speleothems are strong evidence of emergence and confirm inferences of karstification based on seismic reflection profiles and multibeam echo-sounder data over Resolution and other Pacific guyots. Furthermore, the depth of the dissolution, 62 mbsf at Site 867, combined with the nearly 100 m of limestone relief above the site in the guyot center, together imply a fall in relative sea level of at least 160 m. Second, the cores from Sites 867/868 contain much less reefal material than expected. The perimeter mound, once thought to be a reef, may be only a perimeter island chain instead. Furthermore, the volume contribution from reefs to the building of the carbonate platform atop the guyot may be smaller than previously thought.

BACKGROUND AND SCIENTIFIC OBJECTIVES

Sites 867/868 (proposed Site Hue-B) are located atop Resolution Guyot in the western Mid-Pacific Mountains, at 21°20.96'N, 174°18.58'E and 21°21.17'N, 174°18.56'E, respectively (Fig. 1). The two sites are situated at the outer rim of the guyot summit on the perimeter mound (Site 867) and just outside (Site 868) the mound (see "Site Geophysics" section, Site 866 chapter). Prior to drilling, it was assumed that this mound was the youngest Cretaceous fringing reef on the guyot platform.

Along with Site 866, Sites 867/868 were conceived as a part of a transect across a Mid-Pacific Mountains guyot. DSDP Site 463, located approximately 24 nmi (44.4 km) to the east, provided a record of sediments shed by the guyot into the adjacent basin (Shipboard Scientific Party, 1981). Site 866 provided a record of sedimentation in the lagoon behind the perimeter mound. The picture was completed with a hole on the perimeter mound to sample the supposed reef, which would have contributed sediments to both lagoonal and basinal sites. Proposed Site Hue-B was envisioned as a single, shallow-penetration (approximately 300 m) hole, deep enough to sample the perimeter reef through the expected karstified interval.

The profile across the edge of Resolution Guyot (see Fig. 6, Site 866) is similar to profiles across many other Pacific Ocean guyots. Perimeter mounds are common and have been routinely interpreted as fringing reefs (van Waasbergen and Winterer, in press). Thus, the results of Site 867/868 have implications not only for Resolution Guyot and the Mid-Pacific Mountains, but also for Cretaceous guyots in many chains scattered across the Pacific.

Site Selection

Although only a single hole was planned for the perimeter mound of Resolution Guyot (Site Hue-B), drilling results from Sites 865 and 866 showed that a large time gap existed between the formation of the youngest reef atop Mid-Pacific Mountains guyots and the deposition of any permanent pelagic cover. A terrace appears in many places around the perimeter of the guyot, typically 30 m deeper and a few hundred meters outside the perimeter mound. We thought that this terrace might be a reef or wave-cut terrace formed during a relative sea level lowstand, so it might be able to shed light on the missing chapter in the guyot history. Consequently, an extra hole was planned for the terrace near Site Hue-B.

Sites 867/868 are not at the precise proposed location of Site Hue-B, but 1.2 and 1.0 nmi (2.2 and 1.9 km), respectively, to the southeast. Because the perimeter mound and terrace are lineated along the rim of the summit, it was reasoned that most any location on the

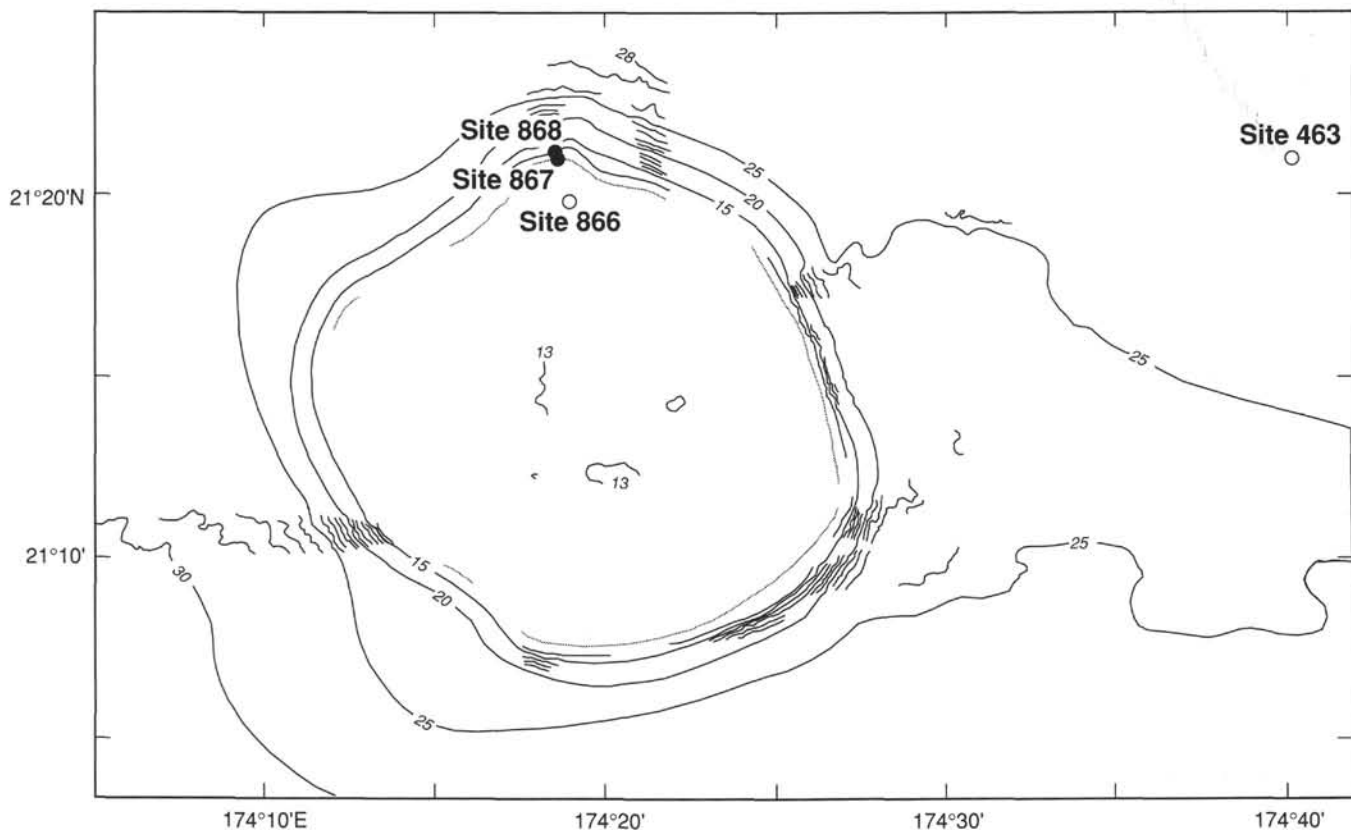


Figure 1. Bathymetry of Resolution Guyot. Bathymetric contours at 100-m intervals where SeaBeam multibeam echo-sounder coverage was available. Heavy contours are at 500-m intervals and include data acquired during pre- and post-drilling surveys aboard the *JOIDES Resolution*. Contour labels in hundreds of meters. Gray line shows the location of the perimeter mound. Sites 867 and 868 are shown by a filled circle; Sites 866 and 463 (DSDP Leg 62; Shipboard Scientific Party, 1981) are denoted by open circles. Site-survey data were acquired in 1988 during Leg 10 of the Roundabout Expedition of the *Thomas Washington* of Scripps Institution of Oceanography.

rim would produce similar results. Consequently, the ship was moved northward by thrusters from Site 866 to the top of the mound nearby to drill Site 867. Likewise, Site 868 was occupied by moving the ship about 400 m northward to the terrace near Site 867. The sites are only about 400 m apart, but because of the shallow water depth, separate beacons were required by ODP policy, which necessitated different site numbers. Because of the proximity of the two sites in space and scientific theme, they are described in a combined report.

Drilling Objectives

The location of Sites 867/868, on the northern perimeter mound of Resolution Guyot, was selected to achieve the following broad goals:

1. Sampling the likely source material, in situ, of sediments drilled at nearby Site 463, where the oldest sediments are redeposited reef debris interstratified with late Barremian pelagic sediments;
2. Learning about the structure and evolution of Cretaceous reefs;
3. Dating the uppermost limestones of the carbonate platform for constraint on the cause(s) of cessation of platform growth and drowning; and
4. Determining the magnitude of emergence and subaerial exposure for comparison with world-wide sea-level curves.

In addition, specific drilling objectives were as follows:

5. To examine the shallow-water carbonate platform biota for comparison with other guyots and carbonate platforms of like age;

6. To examine mineralization and cavity fillings of the upper surface of the exposed shallow-water limestone;

7. To study the diagenetic history of guyot platform carbonates;

8. To obtain data about seismic wave velocity and densities in Cretaceous platform carbonates for use in the interpretation and correlation of seismic reflection and refraction data from Pacific guyots;

9. To collect a suite of downhole logs to illuminate the structure, stratigraphy, and composition of the carbonate platform limestones; and

10. To compare geochemical and isotopic signatures of the carbonate reef for comparison with other similar sediments.

Objectives Addressed and Accomplished

As detailed in various sections of this site report, preliminary shipboard study of the samples and downhole logs collected at the site suggest that most or all of the objectives can be met by further post-cruise studies. Stratigraphic objectives (Objectives 1 and 2) were addressed by detailed examination of sediment textures, structures, compositions, and fossil content. Shipboard age data from macrofossil and microfossil studies are preliminary, but place constraints on the age of the cored material. Furthermore, shore-based strontium-isotope studies should help to refine and confirm these ages. Downhole logs were valuable as an aid for reconstructing the stratigraphy because they provide a continuous record of physical and chemical properties to be used as a framework into which the recovered samples can be fitted.

Objectives 3, 4, and 6, understanding karstification and drowning, were pursued by studying the limestones drilled at Sites 867/868.

Detailed lithologic and chemical analyses of these highest shallow-water limestones were used to infer the extent of karstification and the processes that lead to the demise of the carbonate platform. Once again, downhole logs were important, this time as a tool for giving a record of mineralization in these limestones. Paleontological and strontium isotope studies should yield age constraints on the country rock and the cavity fill sediments.

Objective 5, analysis of biotic assemblages, will continue onshore by macroscopic and microscopic examination of samples and thin sections. Fossils will be compared with the known global distribution of Cretaceous carbonate platform biota.

The diagenetic, isotopic, and geochemical signatures of Cretaceous platform carbonates (Objectives 7 and 10) will be addressed by detailed petrographic examination of thin sections combined with petrologic and isotopic analyses of rock compositions. Downhole logs will be used for additional information about composition and stratigraphic framework. Other properties, such as paleomagnetism, may also yield constraints on diagenetic processes and timing.

Objective 8, the derivation of velocity and density vs. depth data for seismic interpretation, was approached from two directions. One method was to obtain downhole logs of in-situ sonic wave velocity and density. The other method was to perform complementary measurements in the recovered cores.

Downhole logs, acquired to meet Objective 9, proved valuable for interpreting the drilling results at previous sites; thus, obtaining a similar set of data at Site 867 was a high priority. The geophysical tool string was run to gather bulk physical properties (sonic velocity, gamma-ray scatter, bulk density, resistivity). The FMS was also run to obtain a high-resolution resistivity map of the borehole wall for structural and porosity studies.

OPERATIONS

Transit to Site 867

Because the distance from Site 866 to planned Site 867 was only about 2 km, and because we had decided to use the same diamond coring system as was used for Hole 866B, the ship transited between the two sites with the drill pipe hanging beneath the ship about 100 m off the seafloor and with the acoustic beacon at Site 866 as a reference. The ship crabbed northward at a speed of about 0.1 kt, using both the main propulsion system and the after thrusters (to reduce noise at the 3.5- and 12-kHz transducers used for echo sounding). A strong current carried the ship a little west of the planned line of progress, but the echo sounders showed the expected characteristic perimeter mound near the edge of the guyot along our actual course. After passing the crest of the mound, the ship was backed down a few tens of meters toward the crest and a beacon dropped.

Coring Operations at Site 867

Two holes were drilled at Site 867. The first, Hole 867A, was spudded with the diamond coring bit at 1930 UTC, April 24, 1992. The seafloor was very firm, and coring proceeded at a slow rate commensurate with the fact that the BHA was not yet even partly buried and supported by the surrounding hole walls. One core was taken to a depth of 10 mbsf, where only 7 cm of rock was recovered, but when the core barrel for the second core was lowered, it failed to reach the latch point in the bit and circulation appeared to be blocked, perhaps by an obstruction. The core barrel was retrieved, the pipe was raised off the seafloor, and circulation was restored. Another core barrel was sent down, to spud in a new hole, but it simply shot out of the end of the drill string: the bit had been lost. The drill pipe was tripped, and we discovered that the break was at the joint between the bit-sub and the outer core barrel. We also saw that several joints in the BHA had been deformed by the stress of working in the hard formation at shallow penetration depths.

The diamond system and its BHA were set back and a new BHA was assembled, this time with the polycrystalline (PDC) bit, which features diamond-set, lathe-chisel-like insets in the face of the bit that tend to scrape the rock and move cuttings to the outside. This bit had not been tried before on *JOIDES Resolution*, but its good record when coring in hard limestone formations on land provided reason for us to give it a try.

Hole 867B was spudded in at 0615 UTC, April 25, and coring proceeded with good recovery (average 29%) to a depth of 76.8 mbsf (Table 1). In one interval, from 25 to 33 mbsf, the drill pipe appeared simply to drop freely, as if we had entered a cavern, or a series of caverns having only thin separating floors. We began to see that the strata being recovered were becoming more and more of lagoonal facies, like the strata at Site 866, as the bit progressed. Given also that the coring rate was slowing to about 1.5 m/hr in the last 10 m, we elected to abandon the site after obtaining a set of downhole logs. We needed these logs to learn more about the gross structure of the rocks that had been penetrated and partly cored. The evidence of caverns and the possibility that the extent of phosphate mineralization might be determined from a gamma-ray log made logging appear to be worth the extra time needed, in spite of the short length of hole available (about 55 m) below the bottom of the BHA, held at about 20 mbsf.

Because the PDC bit could not be released in the hole, a round trip was necessary to change to a logging bit. Before making the round trip, a television camera was lowered to see what conditions were for reentering the hole. The seafloor was peppered with small rocks, with white sediment in between. A trail the width of the bit could be discerned spiraling toward the hole. The hole was neat and round and only about 40 cm in diameter, with no signs of caving. The ODP Operations Superintendent had already decided to fabricate a tapered metal sleeve about 60 to 75 cm in diameter and 2 m long, and this was slid down the drill pipe, where its lower end embedded itself firmly in the hole. The PDC bit was then tripped out, and the logging-bit BHA lowered.

Logging Operations at Site 867

Upon reentry, the drill pipe was lowered to 16.3 mbsf. The shallow depth of the hole (76.8 mbsf) precluded the use of the conventional tool strings, therefore four short tool strings were used. The heavy compensator was not used during any of the logging runs.

The first tool string consisted of the gamma-ray tool on the bottom and sonic tool on the top. Logs were recorded to 76.1 mbsf in both downward and upward directions. The second logging run was made with the gamma-ray and resistivity tools. Logs were recorded in a downgoing and upgoing direction from 76.6 to 16.3 mbsf. The third tool string consisted of the gamma-ray, neutron porosity, and lithodensity tools. Logs were recorded in an uphole direction from 76.5 mbsf to the base of the pipe. The last tool string deployed consisted of the gamma-ray, FMS, and inclinometer tools. Log data were recorded in an uphole direction from 76.4 to 16.3 mbsf. After the tool string was rigged down, the logging bit was tripped out, and Hole 867B was abandoned.

Transit to Site 868

The transit from Site 867 to Site 868 was made using the acoustic beacon at Site 867 as a reference. The ship steamed slowly (about 0.1 kt) north using the main propulsion and the after and forward (but not the midships) thrusters. The distance was only about 500 m, and the borehole television camera viewed the sea bed as the ship progressed. Close to Site 867, the sea bed was nearly flat and mainly blanketed with white ooze, with scattered small rocks. The seafloor gradually deepened, and at a distance of about 300 m north of Site 867, the seafloor slope steepened northward, and its color changed to gray (this may be because the camera was farther above the bottom). At a

Table 1. Coring summary for Holes 867A, 867B, and 868A.

Core no.	Date (April, 1992)	Time (local)	Depth (mbsf)	Length cored (m)	Length recovered (m)	Recovery (%)
Hole 867A						
1M	24	2145	0.0–10.0	10.0	0.07	0.7
Coring totals				10.0	0.07	0.7
Hole 867B						
1R	24	0900	0.0–8.1	8.1	3.20	39.9
2R	24	1050	8.1–15.1	7.0	1.91	27.3
3R	24	1325	15.1–18.1	3.0	1.02	34.0
4R	25	1800	18.1–24.5	6.4	4.70	73.4
5R	25	1830	24.5–33.9	9.4	0.22	2.3
6R	25	1920	33.9–43.2	9.3	0.55	5.9
7R	25	2000	43.2–52.5	9.3	0.28	3.0
8R	25	2210	52.5–61.8	9.3	1.88	20.2
9R	26	0020	61.8–66.4	4.6	1.65	35.8
10R	26	0230	66.4–68.4	2.0	1.37	68.5
11R	26	0425	68.4–71.4	3.0	0.85	28.3
12R	26	0700	71.4–75.3	3.9	3.34	85.6
13R	26	0830	75.3–76.8	1.5	1.39	92.6
14B	26	1500	76.8–76.8	0.0	0.07	70.0
Coring totals				76.8	22.46	29.2
Hole 868A						
1R	27	2045	0.0–8.0	8.0	1.65	20.6
2R	28	0045	8.0–11.1	3.1	2.11	68.0
3R	28	0430	11.1–13.1	2.0	1.98	99.0
4R	28	0845	13.1–17.2	4.1	2.35	57.3
5R	28	1330	17.2–20.3	3.1	1.31	42.2
Coring totals				20.3	9.40	46.3

distance of about 350 m, the sea bed was again flattish, but at a depth about 25 m deeper than at the 300 m distance. The bottom here was seen to be covered by large platelike slabs, making a slightly rough pavement, with scattered narrow spaces or holes between plates. At a distance of about 490 m north of the beacon at Site 867, and a point thought to be within about 50 m of the break in slope that marks the outer limit of the guyot platform, we dropped a beacon to mark Site 868.

Coring Operations at Site 868

Only one hole was drilled at Site 868, and this only to a depth of 20.3 mbsf.

Because the PDC bit had achieved good recovery rates at Hole 867B, and because we were interested in obtaining good samples from strata close to the edge of the guyot platform, we elected to use again the very same PDC bit used at the previous site, recognizing that coring might go slowly and that our allotted time on Resolution Guyot was fast running out. The bit was the only one of its kind aboard the ship, and, indeed, showed some signs of wear, but this was judged not to be serious.

The spud-in of Hole 868A went slowly: the drill advanced only 8 m in 9.5 hrs. We thought that we may already have broken a record for the shortest hole with the least recovery at Hole 867A and did not want to establish yet another (worst) record. The core recovery over the entire section drilled averaged about 46%, and the quality of the samples recovered was excellent and added significantly to our understanding of the anatomy of the guyot and its sedimentary facies. On the other hand, penetration rates became so slow—the last 3.1 m took 5.75 hr, or at the rate of about 0.5 m/hr—that we reasoned the bit must be nearly worn out. In the end, we simply ran out the clock and stopped coring operations when it was the scheduled time to pull out to begin the departure survey and transit to proposed Site Syl-3.

When the bit was retrieved from the drill floor, the wear was evident, though it still did not appear markedly different from its condition at the beginning of Hole 868A. Inspection of the drill collars showed some cracking, and it became clear that we would have been forced to stop coring in a short time in any event.

Departure Survey of Resolution Guyot

On departing Site 868, after picking up all the beacons from Sites 868, 867, and 866, seismic gear and the magnetometer were streamed and a zigzag survey conducted to define the northwestern boundary of the guyot and to obtain wide-angle sonobuoy and magnetic lines across the guyot, in a nearly north-south direction. The results are described in the “Site Geophysics” section (Site 866 chapter).

LITHOSTRATIGRAPHY

Lithologic Units

Lithologic units have been defined by characteristics such as color, carbonate and phosphate contents, fossil and particle constituents, lithification, and structure. The sequence was divided into two major lithologic units: (1) yellowish-brown phosphatized and manganese-impregnated foraminiferal nannofossil limestone; (2) white shallow-water limestones of variable facies that contain a fauna of rudists, other bivalves, sponges, gastropods, and corals and whose characteristic feature is the presence of cavities filled with phosphatic and nonphosphatic sediments and speleothemic calcitic cement (Fig. 2).

Unit I

Interval 143-867B-1R-1, 0–29 cm
Depth: 0–0.29 mbsf
Age: Eocene

Unit I consists of white and yellowish-brown foraminiferal nannofossil limestone, heavily replaced and impregnated with phosphate and covered with manganese dendrites. Within the sediment abundant, but badly preserved, planktonic foraminifers and rare nannofossils can be seen; crystals of presumed carbonate fluorapatite are visible within this fine-grained material. Locally, the phosphatic material is present as millimeter-scale, rounded brown clasts. The contact with the underlying shallow-water limestones is marked by a surface stained with manganese oxyhydroxides (Fig. 3).

Unit II

Core 143-867A-1R
Depth: 0–10.0 mbsf
Age: Albian

Interval 143-867B-1R-1, 29 cm, to Core 143-867B-14R
Depth: 0.29–76.8 mbsf
Age: Albian

Cores 143-868A-1R to -5R
Depth: 0–20.3 mbsf
Age: Albian

Unit II is a succession of floatstones, rudstones, grainstones, packstones, wackestones, and minor mudstones containing variable amounts of skeletal material, including rudists, sponges, and corals. The carbonates are noticeably vuggy, with many partially filled cavities. Some cavities may be of meter-scale, as at one level, a section of about 9 m gave no resistance to the drill string. In Subunit IIA, phosphatic sediment is a constituent of these fills; in Subunit IIB, it is not.

Subunit IIA

Core 143-867A-1R
Depth: 0–10.0 mbsf
Age: Albian

Intervals 143-867B-1R-1, 29 cm, to -4R-1, 20 cm
 Depth: 0.29–18.30 mbsf
 Age: Albian

The diagnostic feature of this unit is the presence of smoothly sculptured centimeter-scale cavity systems that contain multiple generations of internal sediment (mudstone) of differing colors and compositions, the most prominent of which is a dark-brown fine-grained phosphatic material (Fig. 4). Around these cavity systems, one can see commonly a zone of phosphatization recognizable by a diffuse brown pigmentation. Many of the cavities contain residual void space at the top. Using the same rationale as was used to divide a subunit on Allison Guyot (Site 865), where a zone of high gamma-ray values was attributed to pervasive penetrative phosphatization, that part of the section in Hole 867B that is phosphatized to a substantial degree was assigned to Subunit IIA. The base of the subunit is taken at the base of the lowest cavity that contains phosphatic sediment observed in the core. This level corresponds well with a reduction in the gamma-ray intensity, as seen in the downhole logs (see "Downhole Measurements" section, this chapter) and with the decrease in apatite content, as determined from XRD studies. However, in terms of the broad spectrum of primary carbonate depositional facies, Subunit IIA differs little from Subunit IIB, and the primary sedimentary facies for both subunits are described in the "Subunit IIB" section (this chapter).

Subunit IIB

Interval 143-867B-4R-1, 20 cm, to Core 143-867B-14R
 Depth: 18.30–76.8 mbsf
 Age: Albian

Subunit IIB is characterized by the presence of coarse-grained intervals of floatstone to rudstone interbedded with finer-grained facies of wackestone, packstone, and grainstone. Some of these coarse levels reach 40 cm in thickness and commonly exhibit a fining-upward grain-size distribution. The coarser-grained sediments are composed of shell fragments (mainly of caprinid rudists and nerineid gastropods), intraclasts, and peloids. Fragments of corals, bryozoans, echinoids, and red and green algae are scattered. Many shell fragments and intraclasts are blackened, and most of the particles have been bored and superficially micritized. Floatstone and rudstone levels have been recovered in Cores 143-867B-1R to -4R and again in Cores 143-867B-8R, -11R, and -12R.

Peloidal grainstones displaying low-angle planar stratification and keystone vugs occur in Core 143-867B-4R; ooid sands occur in Core 143-867B-6R. The finer-grained packstones and wackestones contain gastropods, bivalves, rare coral fragments and oncooids, peloids, and black pebbles. Recognizable large rudist fragments were encountered in Cores 143-867B-1R, -4R and -7R. The specimen in the Interval 143-867B-1R-1, 80–95 cm (Fig. 5) contains two separated valves, the larger having its long axis approximately vertical, possibly in life position. Some other large bivalves (*Gervillia* and oysters) also were found in life position. Miliolids, other benthic foraminifers, and ostracods are locally abundant (i.e., in Interval 143-867B-2R-1, 100–111 cm); dasycladacean algae are scattered. Bioturbation of these facies is common. Large, centimeter-sized burrows cut horizontally or obliquely through the sediment, and many of these are filled with greenish wackestone or packstone. Burrow fills are locally brecciated (Fig. 6). Algal laminites and bird's-eye vugs occur in Core 143-867B-12R.

The cavities observed in Subunit IIA are also abundant in Subunit IIB, but they contain only minor amounts of internal calcareous sediment and precipitated calcite (Fig. 7). They measure from a few millimeters to several centimeters across and have either resulted from irregular packing of large clasts, or represent dissolution channels. White to yellow calcite cements that locally attain the status of speleothems commonly line the cavity walls. In some cavities, the

lining is clearly botryoidal on the upper surface, whereas the lower surface bears only a laminar crust. A coating of coarse calcitic spar covers some of the speleothems. It was in this subunit that the lack of resistance to the drill string suggested the presence of a nearly 9-m-deep cavity (Core 143-867B-5R).

Subunit IIC

Cores 143-868A-1R to -5R
 Depth: 0–20.3 mbsf
 Age: Albian

Subunit IIC occurs only in Site 868 and is characterized by the presence of several intervals of boundstone. In terms of its stratigraphic position with respect to Subunit IIB, given the somewhat greater depth of Site 868 relative to Hole 867B, Subunit IIC should be considered a time equivalent of Subunit IIB. The boundstone (bafflestone) is principally constituted by different types of sponges in growth position that rest on erosion surfaces and form colonies up to 20 cm high. Several of the observed sponge colonies are not in a vertical position, which may be because of their having been overturned by storms, or by having grown on an irregular seafloor having cliffs and overhangs (Fig. 8). Sponge types include branching forms with nonsegmented tubes 1 to 2 cm in diameter (Fig. 8), branching forms with segmented tubes, 5 to 7 mm in diameter, fanlike forms having fine, elongate canals 0.2 to 0.5 mm in diameter (Fig. 9), and massive forms with a branching pattern of small canals about 1 mm in diameter. One sponge type generally predominates in a given sequence, but can be replaced vertically by another type. Sponge tubes are commonly covered by sessile foraminifers and filamentous algae, with the latter contributing to the stabilization of the bioherms (cf. Flügel and Steiger, 1981). Binding with filamentous algae is also significant in many of the associated bioclastic sediments.

The boundstone is interbedded with floatstone and minor grainstone rich in requieniid and caprinid rudists, high-spired gastropods, sponge fragments, possible chondrodontid oysters, and oncoidally coated particles of millimeter-scale. Much solutional porosity exists, and spar-lined voids are common. In Section 143-868A-1R-1, a speleochemic interval is present in which the host grainstone contains multiple generations of fine-grained internal sediments developed as white, brown, and reddish laminae. The microfacies of this internal sediment is partly peloidal with a microsparite matrix and grades up into micrite. Possible keystone vugs are present in Sample 143-868A-5R-1, 55–56 cm. The basal 70 cm of Section 143-868A-3R-1 is noticeably reddened and appears to have been mixed with internal sediment.

Interpretation of Sedimentary Environments and Diagenesis

The general facies evolution of Hole 867B implies a general opening of the depositional environment, from restricted lagoon to foreshore and shoreface. This trend was modulated by smaller transgressive-regressive cycles, resulting in meter-scale sequences that can be recognized in many intervals of the recovered material. An idealized sequence summarizing many of the facies observed in Subunit IIB is presented in Figure 10. Peloidal packstones with bivalves in life position and evidence of bioturbation suggest a well-oxygenated environment below a fair-weather wave base. Scattered layers of shell debris and black intraclasts indicate storm activity. The sequence shallows upward into a foreshore setting, where a shell layer may correspond to the subtidal berm, above which occurs a grainstone with planar beach lamination and including keystone vugs in its upper part. The top of the beach facies is then capped by a fining-upward succession of reworked shell debris and intraclasts, including abundant blackened fragments, which can be interpreted as a storm wash-over. The primary erosive base may be overprinted by post-deposi-

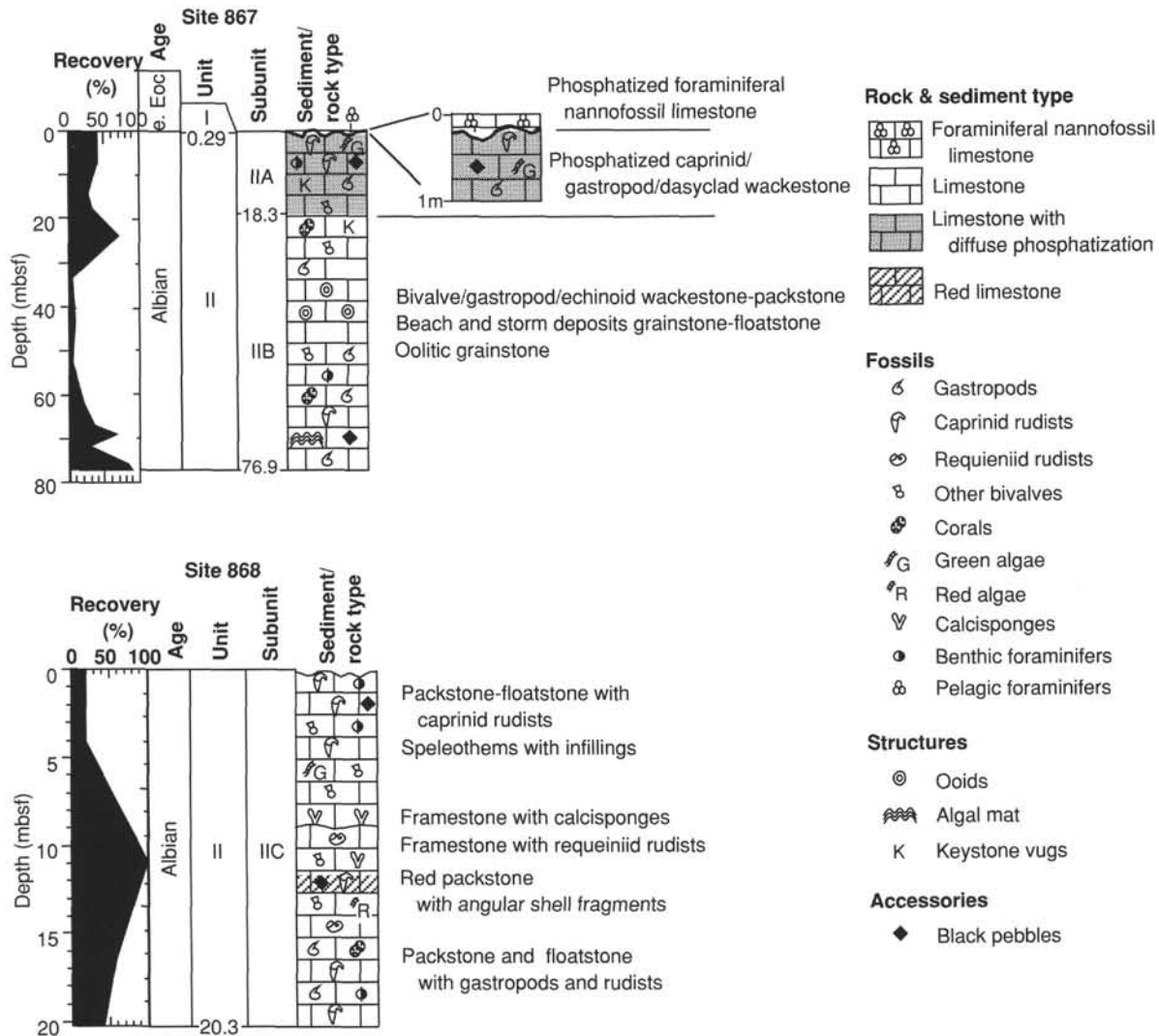


Figure 2. Interpretive stratigraphy of Holes 867B and 868A.

tional burrowing (Fig. 6). The overlying packstones and wackestones contain a lagoonal fauna and flora, indicating a protected depositional environment. Occasionally, the lagoon shallows upward into intertidal flats.

The facies suggest the presence of a beach barrier protecting the late Albian lagoon from the high-energy influence of the open ocean. Storm deposits are common, especially in the upper part of Hole 867B, and may correlate with the coarse-grained intervals in Subunit IIIA of Site 866.

The range of sedimentary environments reconstructed for Subunit IIC is the same as for Subunit IIB: rudistid facies, storm deposits, and reddish internal sediment are characteristic features, the last implying emergence. The most conspicuous feature of this subunit is the presence of calcisponge communities that probably developed near or below the fair-weather wave base in an open-marine environment. A summary of some of the observed depositional sequences in Core 143-868A-2R is given in Figure 11. Erosional surfaces at the base of redeposited layers imply scouring of soft sediment by storms, whereas surfaces truncating shell fragments suggest erosion and dissolution of a cemented substrate during periods of sediment bypass. Locally, organic (?algal) encrustation and *Lithophaga*-type borings occur. The sponge bafflestones developed preferentially on erosion surfaces that presented hardgrounds or firmgrounds on which the fauna could

anchor. Expansion of these sponge bioherms was probably forestalled by frequent storm erosion or by rapid burial in sediment. Locally, pervasive binding by filamentous algae of the skeletal carbonate sands implies periods of reduced water circulation and possibly nutrient excess (Hallock and Schlager, 1986).

The most obvious diagenetic feature of Unit II is the development of solution cavities and their subsequent filling with a variety of internal sediments, some of which are phosphatic. The occurrence of speleothems in the lower part of Subunit IIB suggests that precipitation of dripstone took place within the lower vadose zone (Esteban and Klappa, 1983). Given that speleothems occur at least as deep as Interval 143-867B-9R-1, 57–64 cm, at a depth of more than 60 mbsf, it follows that the atoll was exposed at least to this height above sea level during karstification.

After the drowning of Resolution Guyot, conditions clearly remained essentially nondepositional in the area of the drill sites for many millions of years, and not until the Eocene was any permanent pelagic cover developed. This cover is now comprehensively phosphatized. Dating the entry of phosphatic sediment into the cavities that permeate the top of the atoll cannot be readily accomplished; it could equally be Cretaceous or Tertiary. The fact that phosphatization of the upper part of the shallow-water section is not limited to passive filtration of sediment into void space, but also involves replacement

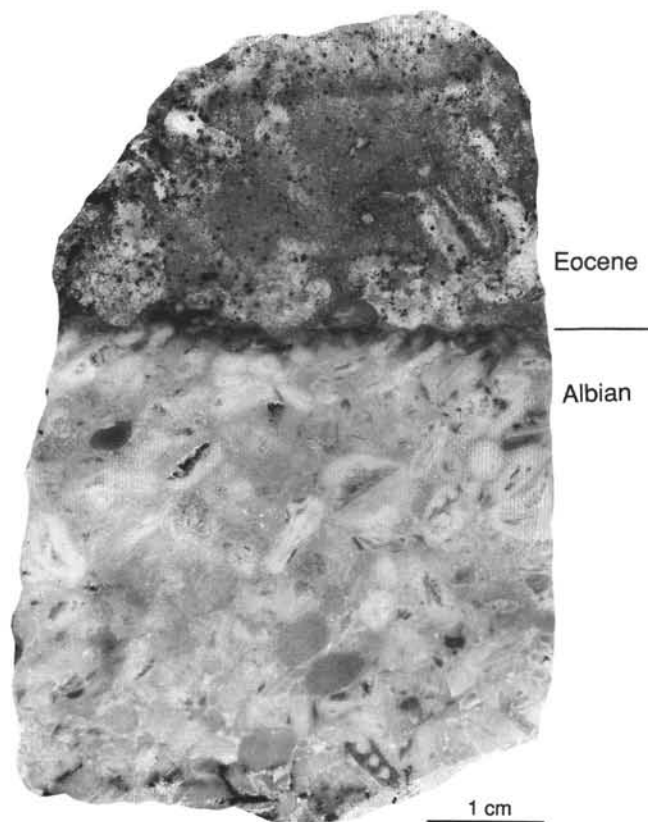


Figure 3. Contact between upper Albian shallow-water floatstone and Eocene phosphatized foraminiferal nanofossil limestone (Interval 143-867B-1R-1, 0–13 cm).

of the carbonate matrix surrounding the conduits, shows that solutions charged with phosphate may have circulated within an interconnecting cavity system.

The thin cap of phosphatized foraminiferal nanofossil limestone cored in Hole 867B is missing from the perimeter of the guyot at Site 868, indicating that this area is still nondepositional.

BIOSTRATIGRAPHY

Foraminifers

Hole 867A

Rare, poorly preserved, agglutinated benthic foraminifers were found in Sample 143-867A-1R, 1–3 cm, in association with large bivalve and echinoid fragments, nerineid gastropods, solenoporacean and green algae, and rare ostracods. Rudist fragments have been bored by clinoid sponges and are encrusted with green algae. Biogenic lithoclasts contain lithophagid(?) bivalves that have been preserved in their borings. This biologic assemblage, in association with coarse bivalve detritus and smaller, rounded and blackened biogenic debris, suggests a current-swept, shallow-marine environment that was mixed with foreslope sediments during episodic events or storms.

Hole 867B

Cenozoic planktonic foraminifers occur in white pelagic limestone deposited directly on Albian shallow-water limestone or in several intervening thin, millimeter-scale, yellowish-brown pelagic layers on the limestone. The assemblage from the white limestone, examined in thin section, contains moderately to poorly preserved specimens that include *Morozovella quetra*, *Morozovella aragonensis*, *Morozovella formosa*, *Pseudohastigerina wilcoxensis*, *Subbotina*

eocenica, *Acarinina* sp. cf. *A. pentacamerata* and has been assigned to the lower Eocene (Zones P7–P8). An apparently similar, but very rare, assemblage from the several yellowish-brown layers that, in some places, are separated by a single, manganese-stained surface that extends laterally onto the surface of the shallow-water limestone, appears to be the same age.

The shallow-water limestone of Hole 867B contains benthic foraminifers of Albian age. The assemblage includes *Cuneolina* sp. cf. *C. pavonia*, *Nezzazata* sp. cf. *N. simplex*, miliolids, textulariids, and small trochospiral forms. This assemblage is similar to that of the Albian limestone at Sites 865 and 866. Other biogenic constituents include rudist and other bivalve fragments, echinoid debris, gastropods, ostracods, bryozoans, and solenoporacean and dasy-cladacean algae. Two general biofacies were identified in the Cretaceous sequence: (1) high-energy open-marine conditions and storm deposits represented by macrofossil debris in coarse shell detritus, whole and relaminated broken ooids, and blackened and/or coated, rounded grains, and (2) quiescent lagoonal conditions represented by the miliolid-textulariid-cuneolinid assemblage in wackestone. Some of the coarsest shell material occurs in Cores 143-867B-1R and -4R, interspersed with intervals containing more lagoonal material. Predominantly lagoonal material first occurs in Core 143-867B-2R and becomes more abundant downhole; however, it is difficult to determine if environmental conditions generally become more turbulent uphole or if storm effects are more prevalent in the uppermost cores.

Site 868

Cores 143-868A-1R to -5R contain rare benthic foraminifers, assigned to the Albian. The assemblage consists mostly of miliolids, textulariids, and small trochospiral forms. The most useful biostratigraphic indicators include several miliolids that resemble *Moesiloculina histri* in Sample 143-868A-2R-2, 21–24 cm, *Sabaudia* sp. cf. *S. minuta*, *Nezzazata* sp. cf. *N. simplex*, and *Spiroloculina* sp. cf. *S. cretacea* in Sample 143-868A-4R-2, 0–3 cm, and *Cuneolina* sp. cf. *C. pavonia* in Sample 143-868A-5R-1, 137–138 cm.

Depositional environments at Site 868 differ from those of the other shallow-water carbonate sites of Leg 143 in their abundance of algae and sponges, as well as blackened and algal-encrusted bioclastic detritus. Coarse macrofossil debris is common and diverse, while the abundance of benthic foraminifers reaches a minimum for unaltered samples from Allison and Resolution guyots.

Algal boundstone dominates samples from the base of the cored sequence in Cores 143-868A-3R to -5R. Benthic foraminifers consist of rare miliolids, textulariids, and small trochospiral forms, with single specimens of cuneolinids and other agglutinated forms, rare open-marine calcareous species, and more numerous encrusting taxa. Other biogenic material includes common bivalve and echinoid fragments, diverse green algae, scattered sponges, rare solenoporacean and dasycladacean algal debris, bryozoan fragments, and rare-to-few ostracods. Rudist fragments contain clinoid sponge, algal, and other borings. Calcite crusts are found in the algal matrix of Cores 143-868A-3R and -4R.

Samples from Cores 143-868A-1R and -2R consist of packstone and wackestone. Free benthic foraminifers are very rare and are limited to miliolids, textulariids, small trochospiral forms, and open-marine calcareous species, whereas encrusting taxa, such as *Acruliammina*, are often common. Macrofossil detritus continues as below, but with coarser bivalve and echinoid fragments. Binding green algae is absent or rare in the samples; however, calcispheres are abundant in the pelmicrite of Sample 143-868A-1R-2, 36–38 cm.

These facies suggest a shallow, foreslope depositional environment below a normal wave base that shoaled uphole. The algal boundstone biofacies at the base of the section likely formed in the less turbulent water downslope from the platform margin, but above the steep side slopes of the seamount. Species of green algae abounded, and open-

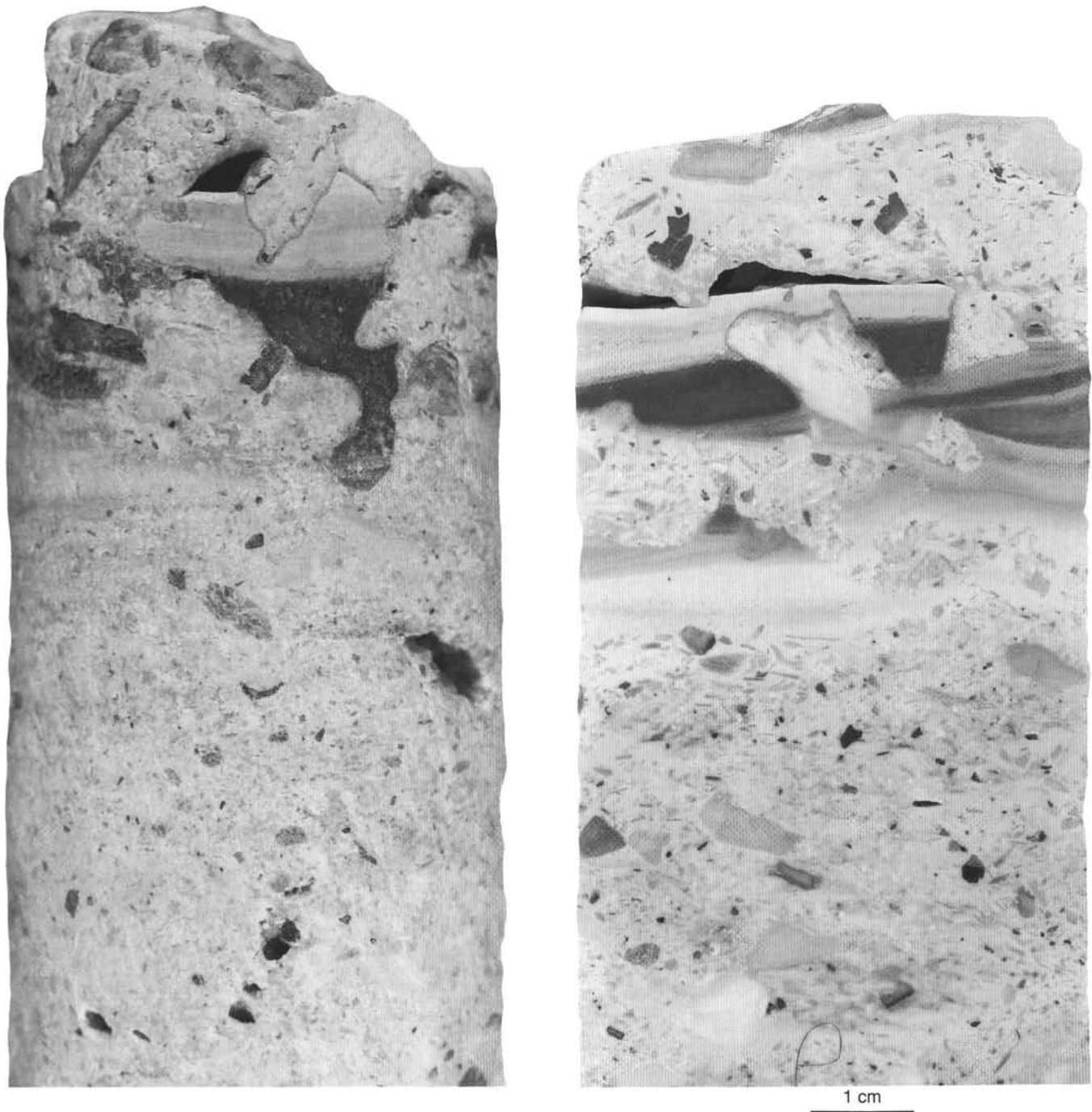


Figure 4. Two photographs of uncut (left) and cut (right) core illustrating cavity system of Subunit IIA with fills of brown phosphatic sediment overlain by laminated light-colored micrite and showing minor residual void space (Interval 143-867B-4R-1, 17–24 cm).

marine calcareous benthic species and questionable small planktonic species were present in limited numbers. The algal biofacies perhaps represents the source of blackened bioclastic grains that were eroded and redeposited upslope during storm events.

Spongelike material within the algal biofacies, and especially uphole in Section 143-868A-2R-1, suggests the presence of sponge thickets upslope from the algal biofacies. Abundant, small, centimeter-scale requeniid rudists occur in Section 143-868A-2R-1 that are associated with calcisponges in a mudstone matrix, indicating that these primitive rudists preferred the muddy, less turbulent habitats

below the higher-energy caprinid-dominated environment that was present in Section 143-868A-1R-1. Finally, the patchy and often muddy caprinid biofacies drilled at Sites 867 and 868 suggests that the platform margin sites were located toward the leeward side of the seamount during the Aptian and Albian.

Rudists

Recognizable large caprinid rudist fragments occur in Cores 143-867B-1R, -4R, -7R, and Cores 143-868A-1R, -2R, and -4R. Preser-

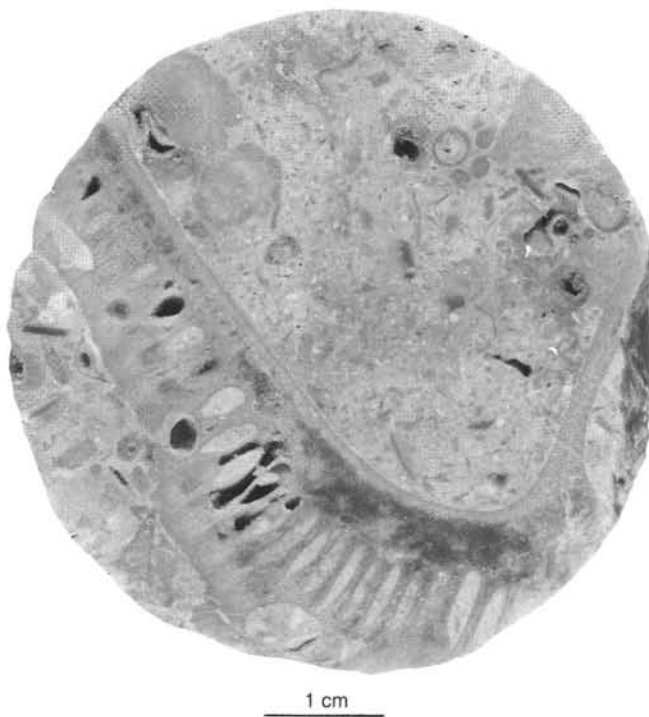


Figure 5. Caprinid rudist (*Planocaprina?*) displaying well-preserved canal structure (Interval 143-867B-1R-1, 85 cm).

vation of most of these pieces has involved the formation of a micritic envelope that seeded on the surface of the aragonitic shell layer. The original boundary of the canals is generally marked by the outer surface of this rind. In some pieces, there has been later void-fill cement between the micritic rind. Where cementation is incomplete, or where the largest crystals have been preferentially eroded, a cavity may have been created between the canals on the outer side. This can give the erroneous impression that, originally, smaller canals alternated between and on the outside of the main row (or, alternatively, that the walls between the canals bifurcate).

Three main types (probably different genera) of caprinid rudists were distinguished at these sites, and one can be further subdivided into two slightly different forms (most likely different species).

Type 1a

This category includes all four specimens from Site 867 and five from Site 868. Most of the description below is based on the large specimen from Sample 143-867B-1R-1, 80–95 cm (Fig. 5), which consists of two separated valves, the larger having its long axis approximately parallel to the core in probable life position. In this piece, the valve diameter probably reaches 7 to 8 cm (although only just over half has been preserved). One valve is at least 10 cm in length and is slightly curved. No obvious protuberances, or keels, are seen on the outside of the valves. No ligamentary structures were observed. An outer zone about 1 cm thick bears one row of thin, pyriform canals. This zone appears to surround the entire margin. The canals start approximately 2 to 3 mm from the outside of the inner wall and continue outward, so that the thin “bottleneck” (now filled in by the micrite envelope) probably extends to the outside wall, for a total length of about 7 mm. At their widest, some canals reach 2 mm, whereas most are 1 to 1.5 mm wide. In general, the length/width ratios are between 5 and 7 for type 1a. No original structure of the canals suggests that the walls bifurcated. The larger valve in Samples 143-868A-4R-1, 105–107 cm, and 143-867B-1R-1, 80–95 cm, shows a bar separating a relatively small access-

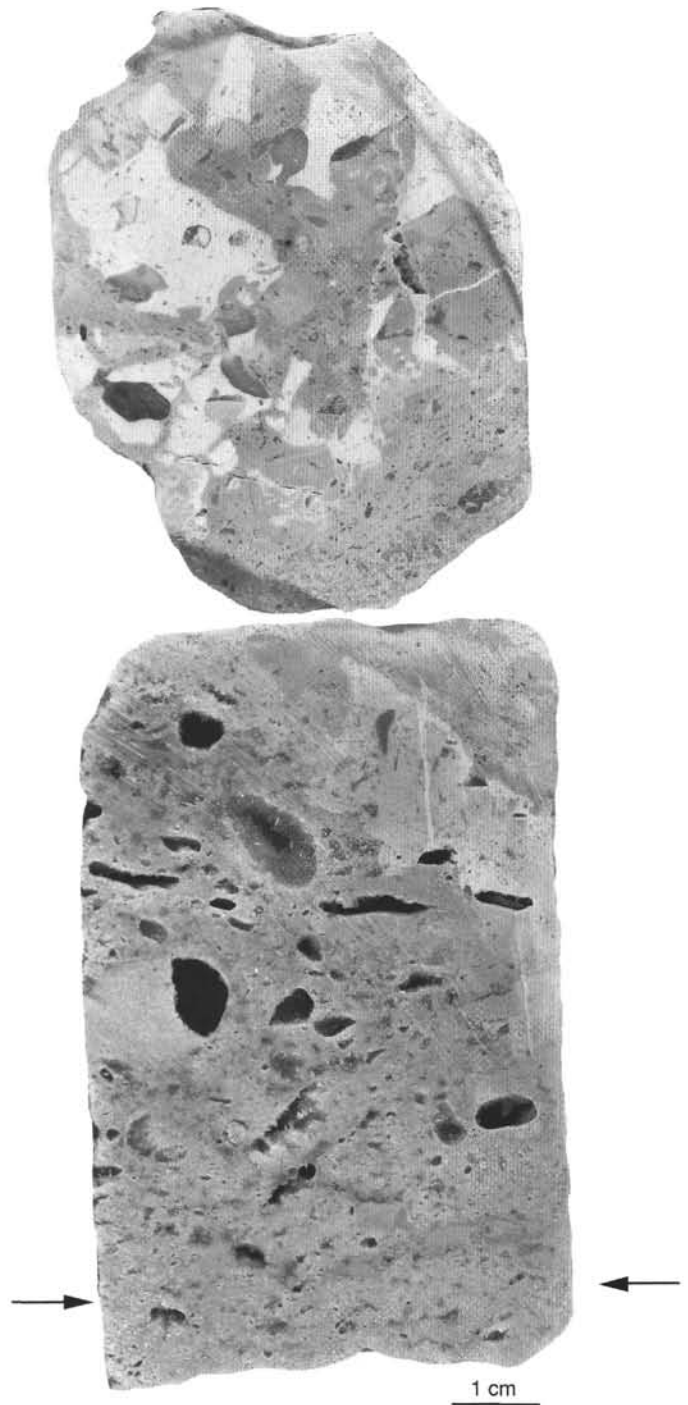


Figure 6. Upper specimen: brecciated burrow system filled with light gray-green wackestone. Lower specimen: burrows penetrating into peloidal grainstone with keystone vugs (arrows) and molds of shell fragments (Interval 143-867B-2R-1, 130–145 cm).

sory cavity from the body cavity. Other pieces having almost complete transverse sections (Samples 143-867B-1R-1, 80–95 cm, and 143-867B-1R-2, 87–90 cm) lack this bar; thus, it seems likely that it is present in only one valve. The specimen from Sample 143-868A-2R-1, 3–9 cm shows that in longitudinal section, some of the canals have regularly spaced tabulae that slope away from the body chamber at a fairly steep angle.



Figure 7. Cavity system typical of Subunit IIB, containing light-colored laminated micrite and substantial void space (Interval 143-867B-9R-1, 57–63 cm).

Type 1b

Specimens from Samples 143-868A-4R-2, 98–102 cm, and 143-868A-1R-2, 0–8 cm, are described as type 1b. This form seems identical to type 1a, except that the canals are relatively broader and more teardrop-shaped (length/width ratios less than 3). The specimen from Sample 143-868A-1R-2, 0–8 cm, is a right valve that shows a conical anterior socket and a central tooth elongated to a ridge in the anterior direction.

The presence of a single row of pyriform canals, which encircles the entire margin of both valves, and the presence of an accessory cavity in one valve (presumably the left valve) suggest that the specimens may belong to *Planocaprina*.

Planocaprina, described by Palmer (1928, figs. 7–8, p. 66–67), has a ligamentary invagination and relatively thin shell layer with teardrop-shaped canals that encircle the margin. The intervening walls supposedly show some bifurcations in the ventral margin, but this is likely a preservational artifact (see above). Similarly, the wall is probably solid with distinct holes, rather than mostly void with a sheetlike lamella defining the external wall, as drawn by Palmer. *Planocaprina*, originally described from Jalisco, Mexico, is found with *Coalcomana* and *Caprinuloidea* of probable late Albian age.

Therefore, it is most likely that type 1 belongs to the genus *Planocaprina*, although no ligamentary invagination was observed in these specimens. The larger size and more rotund outline makes them unlike *P. trapezoides*, and they probably represent two new species of this genus. However, type 1a does have the canal shape of *P. trapezoides*. Type 1b is similar to "*Planocaprina*" sp., as figured by Coogan (1977, pl. 10, fig. 5) from the lower Aptian Sligo Formation of Texas, although Skelton (1982) questioned the identification of this specimen.

Type 2

Three fragments from Samples 143-868-3R-1, 25–32 cm, -4R-1, 7–9 cm, and -5R-1, 27–32 cm, have been assigned to this form, and

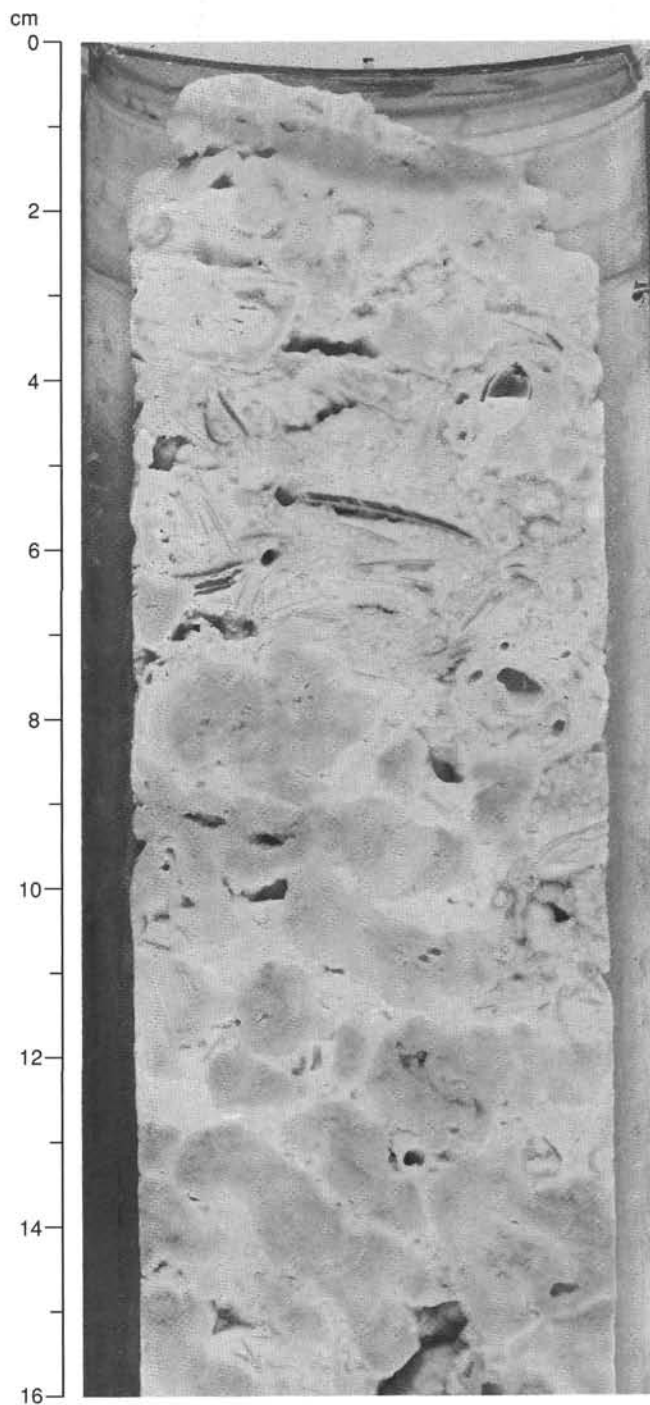


Figure 8. Branching tubular calcareous sponge colony displaying fine canals and growth rings. Growth direction is from left to right in photograph. Interbedded sediment is bivalve-rich, peloidal packstone exhibiting shelter porosity and geopetal fills (Interval 143-868A-2R-2, 0–16 cm).

all are thought to be parts of the shell wall from the cardinal area. The form has rectangular subrounded canals that are rarely subdivided. In one instance, the intervening walls are very thin.

Some similarities exist between these specimens and *Amphitris-coelus waringi* Palmer (1928), now thought to range from the late Barremian to the late Albian (Kauffman et al., unpubl. range chart). For this to be the correct assignment, it would imply that two of the specimens were sections at some distance from the commissure, where the canals are somewhat cemented up and no longer rectangular.

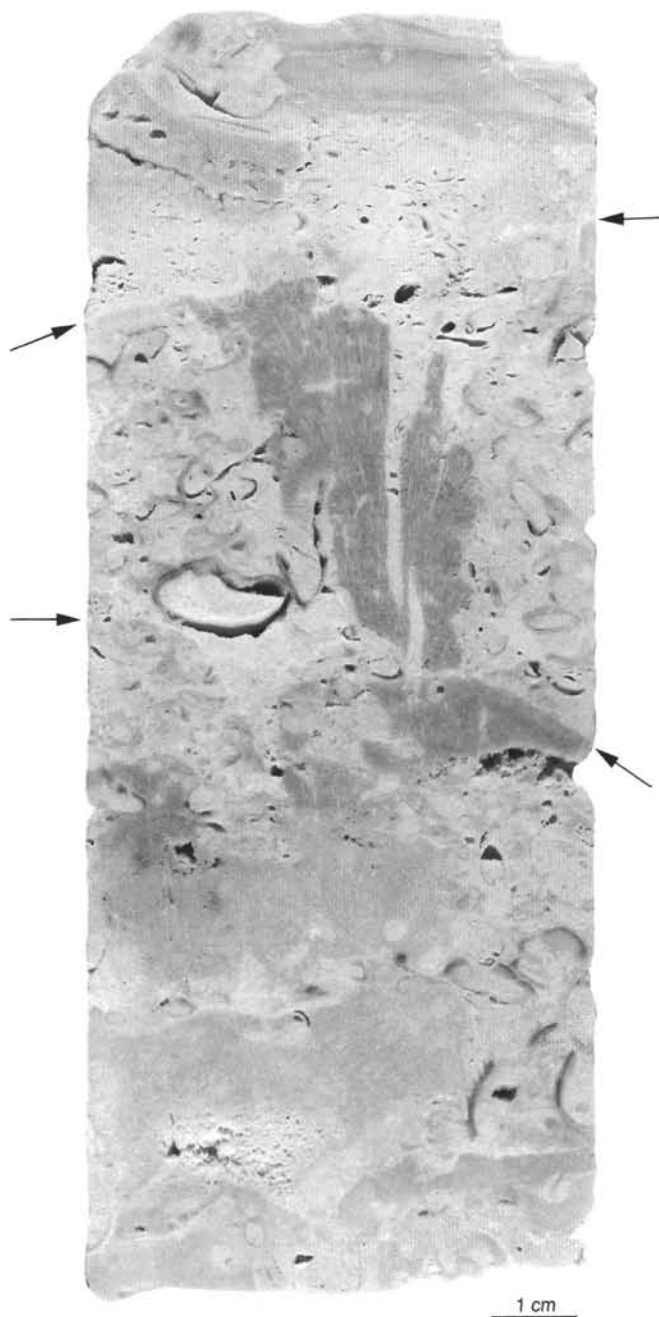


Figure 9. Heavily bioeroded fanlike colony of calcareous sponges. Two erosion/dissolution surfaces cut through the sediment (arrows). The encasing sediment is peloidal packstone with requieniid rudists. Note geopetal void fills (Interval 143-868A-2R-1, 74–87 cm).

lar. The distinctive tripartite division of the main shell into a body cavity and two large accessory cavities, which defines this form, was not observed, and the diagnosis is tentative.

Type 3

Only one example of this form was recovered (Sample 143-868A-4R-1, 94–100 cm; see Fig. 12). It has a very small sediment-filled body cavity (1 cm) compared to the diameter of the valve (5 cm maximum). No canals are seen in the dorsal region, but the specimen has an irregular mosaic of divided canals on one side and sinus,

teardrop-shaped canals on the other. This is an advanced caprinid, possibly *Caprinuloidea*, with a stage of development known only in caprinids from the late Albian and later. Additional specimens will be required to diagnose this specimen further.

PALEOMAGNETISM

Site 867

The magnetic signal proved to be as weak in the limestones recovered from Site 867 as in those measured from previous sites during Leg 143. We measured large (50 cm³ and larger) pieces from the archive halves of Cores 143-867B-1R through -12R as discrete samples in an effort to increase the accuracy of the measurements by increasing sample volumes. The samples were demagnetized in an alternating field (AF) with steps of 0, 5, 10, and 15 mT. Measured intensities were insignificant and well below the noise level of the shipboard cryogenic magnetometer (approximately 1 mA/m).

Site 868

In those parts of Cores 143-868A-1R through -4R that contained red staining, magnetic intensities tended to be slightly higher than those in the cores from Site 867. These intervals exhibit a slight overprint, a negative inclination interpreted as a normal polarity, and a magnetization that does not seem to demagnetize readily at the low fields (0, 5, 10, and 15 mT) applied by the pass-through AF demagnetizing system (Fig. 13). Based on the hardness of this magnetization, in addition to the reddish color of the sediment (see "Lithostratigraphy" section, this chapter), we infer that the magnetic carrier may be hematite.

INORGANIC GEOCHEMISTRY

Interstitial Waters

One sample was taken for interstitial water analysis from Hole 867B (143-867B-1R-2, 29–30 cm). The normal squeezing techniques failed to extract pore water from this sample.

ORGANIC GEOCHEMISTRY

Sixteen samples from Hole 867B and 10 from Hole 868A were analyzed for carbonate content using the Coulometrics carbon dioxide coulometer. Total nitrogen, sulfur, carbon, and organic carbon contents were measured by means of an NA 1500 Carlo Erba NCS analyzer. The procedures used for these analyses are outlined in the "Explanatory Notes" chapter (this volume). The results are given in Table 2.

Inorganic carbon

The calcium carbonate contents are very high, as expected, in the shallow-water carbonate platform facies. Carbonate content in Hole 867B ranges from 98.5% to 100% in most of the samples (Fig. 14). Only Sample 867B-9R-1, 20–21 cm, with 95% CaCO₃, shows a lower value. No lithologic variation seems to explain this difference. In Hole 868A, all the samples contain between 99.5% and 100% CaCO₃ (Fig. 15). The slight variations recorded are not significant because they are in the range of the precision of the coulometer.

Organic Carbon Content

The total organic carbon (TOC) content of selected samples from Holes 867B and 868A is presented in Table 2. Very low TOC values (< 0.3%) are observed in most of the samples, except in Sample 867B-9R-1, 20–21 cm, which contains 0.41% TOC. Total nitrogen and sulfur concentrations were often below the detection limit of the NCS analyzer.

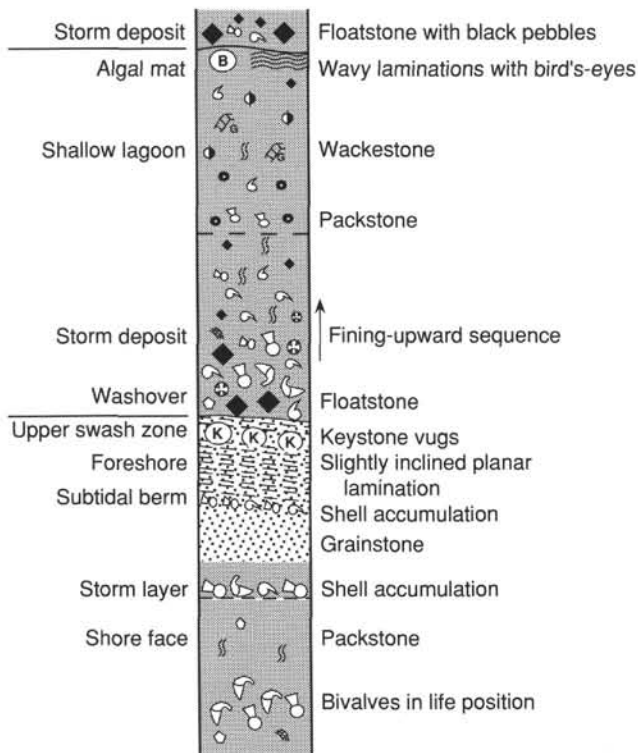


Figure 10. Idealized meter-scale sedimentary sequence characteristic of Subunits IIA and IIB.

PHYSICAL PROPERTIES

Introduction

Sites 867 and 868 objectives were identical to those at Site 866: (1) to measure index properties and P -wave velocities in the lithified carbonate-platform sediments; (2) to identify physical-property units for correlation with Site 866; and (3) to identify lateral correlations or trends in physical properties going from protected lagoonal facies through transitional lagoonal-skeletal margin (Sites 866 and 867) and, finally at Site 868, foreslope to reefal facies. No cover of pelagic sediment was present at either Site 867 or Site 868.

At Site 867, two holes, tens of meters apart, were drilled in the slightly elevated margin (Holes 867A and 867B). Technical problems forced the abandonment of Hole 867A, and time constraints limited the drilling of Hole 867B. Hole 867B reached a depth of 76.8 mbsf in the marginal zone of the carbonate platform at Resolution Guyot. This zone, showing up as discontinuous and irregular reflectors in the seismic record, was supposed to have reefal sediments or shallow-water, skeletal, sand shoals. Sediment recovered in Hole 867B consists predominantly of mollusk-rich (rudists and gastropods) wackestone and packstone, oolitic grainstone, and coarse mollusk-rich rudstones. Hole 868A, drilled in the outer edge ("seaward" of Site 867) of the carbonate platform margin, foreslope to reefal facies, reached a depth of 20.3 mbsf, and sediment recovered consists primarily of (top to bottom) packstone and floatstone with rudists, calcisponge-framestone, and floatstone and mollusk-rich packstone.

In the lithified platform sediment, cored with a PDC bit, P -wave velocity was measured in both longitudinal and transverse directions in cubes (one-in.) as well as in minicores (one-in. diameter). For each pair of horizontal and vertical velocity measurements, the anisotropy was calculated. In addition, index properties, bulk density, porosity, grain density, and water content (% dry weight) were measured. No corrections were made for salt content (see "Physical Properties" sec-

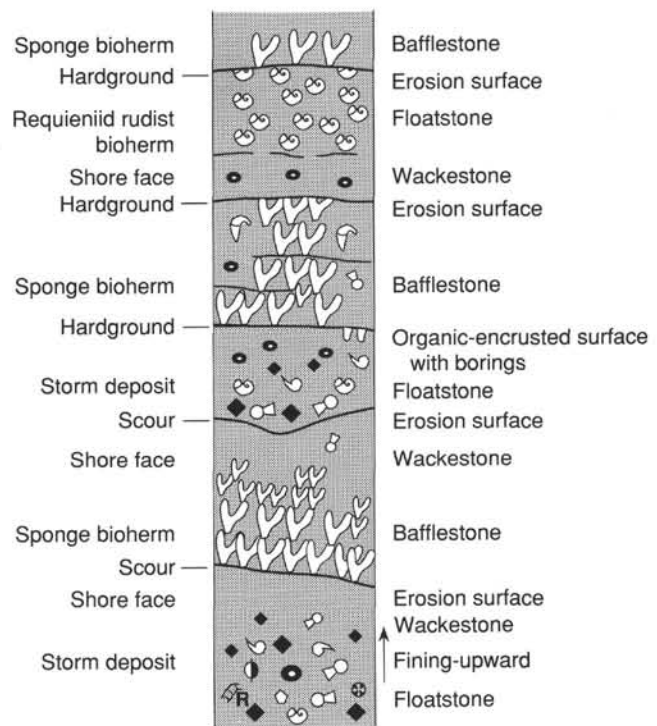


Figure 11. Summary sketch of some of the facies of Subunit IIC (Core 143-868A-2R). The length of the intervals between erosion surfaces varies between 10 and 30 cm.

tion, Site 866 chapter). Owing to low recovery (especially in the interval between 30 and 65 mbsf) and the shallow depth of Holes 867B and 868A, no subdivision into physical-property units was attempted.

Data for Holes 867B and 868A are presented in Tables 3 and 4, showing the index properties and sonic velocity measurements, respectively. Figures 16 and 17 present the correlations among index properties, sonic-velocity measurements, and recovery for Holes 867B and 868A, respectively. Figures 18 and 19 show the correlation among sonic velocity, anisotropy of sonic velocity, and recovery, in higher detail, for Holes 867B and 868A.

Besides a few measurements in the interval from 18 to 35 mbsf, index properties are constant in Hole 867B: bulk density ranges from 2.15 to 2.71 g/cm³, porosity ranges from 4.70% to 38.77%, water content ranges from 1.79% to 22.04%, and grain density ranges from 2.70 to 2.87 g/cm³. Sonic velocity (vertical velocity measured in cubes) varies from 2.88 to 6.52 km/s. Anisotropy of velocity shows more negative values and a narrower distribution of data points in the upper part of Hole 867B (0–35 mbsf) than in the lower part. In the lower part of Hole 867B, the anisotropy data show more scatter and both negative and positive values. Overall, average anisotropy is -3.32% for the entire Hole 867B.

Index properties and sonic velocity measured in Hole 868A show little variation: bulk density ranges from 2.36 to 2.71 g/cm³, porosity ranges from 2.88% to 24.21%, water content ranges from 1.08% to 11.45% and grain density ranges from 2.74 to 2.82 g/cm³. Sonic velocity varies between 4.53 and 6.66 km/s, with an average of 5.94 km/s. Values of anisotropy of sonic velocity are negative, with a mean of -3.32%.

Density-velocity relationships at Site 867 (0–76.8 mbsf) are similar to those in the shallower layers at Sites 865 and 866. Average sonic velocity, vertical velocity measured in cubes, and bulk density (of the recovered sediment) values are slightly higher at Site 867 than in PP



Figure 12. Rudist type 3 from Interval 143-868A-4R-1, 94–100 cm. Identification indeterminate (see text for details).

Unit 2 (0.9–430 mbsf) at Site 866; 5.47 vs. 5.25 km/s, respectively. At Site 868A, sonic velocity varies between 4.53 to 6.66 km/s, with an average of 5.94 km/s, which is even slightly higher than that measured at Sites 867 and 866 (PP Unit 2, 0.9–430 mbsf). Velocity and density data from discrete measurements, however, do not give a representative image of the velocity and density profiles in Holes 867B and 868A. More continuous data from the sonic and density logs may significantly improve the information about the acoustic properties of the marginal zone. Important is the possibility that substantial caverns are present at this site, which may dramatically change the acoustical properties, consequently influencing the quality of the seismic record in the marginal zone of the guyot.

Sonic-velocity data suggest that average sound velocities in the slightly elevated and convex-upward margin (see “Seismic Stratigraphy” section, this chapter), Holes 867A and 868A, are higher than those in the platform interior, Site 866, which may have implications for the interpretation of the elevated structure. Conversion of traveltime into depth-in-meters may thus reduce the apparent height of the elevated rim in the seismic record. The reason for this trend in sonic velocity (and bulk density) may be the increase in intensity of syndepositional to post-depositional cementation and recrystallization in going laterally from the lagoonal facies into the outer-rim reefal facies, corresponding to a change from more muddy sediment to washed sands, and thus a considerable increase in pore-water circulation.

DOWNHOLE MEASUREMENTS

Introduction

Wireline measurements were performed at Site 867 of the in-situ properties of the perimeter-facies sediments of Resolution Guyot. Hole 867B, which penetrated 76.8 m of predominantly wackestones and grainstones, was the only hole logged at Site 867. The base of the drill pipe was kept at 15.5 mbsf during the entire logging operation. Four tool strings were run, including the sonic-gamma-ray, the gamma-ray-resistivity, the gamma-ray-porosity-density, and the gamma-ray-FMS-tool strings. The logs recorded by these tools produced good data. Geochemical logs were not run because of operational constraints.

Reliability of the Logs

Hole size and condition were the most important controls on the accuracy of logs from Hole 867B, and the caliper is the best indicator for these parameters. The hole diameter through most of the logged interval is less than 14 in. (36 cm), slightly greater than the bit size of 10 in. Consequently, over most of the lithodensity tool string run, the pads made satisfactory contact against the borehole wall. On the other hand, the density log does show some swings to unreliably low values (Fig. 20). These swings correlate with the high caliper values that indicate washout in these regions. This loss of strength or cohesion correlates with resistivity and velocity changes that indicate a change in porosity and/or composition. Most other logs do not require pad contact and therefore are less sensitive to changes in the size of the borehole; gamma-ray and resistivity logs probably will change only slightly with post-cruise borehole correction.

The initial sonic logs from Hole 867B exhibited some zones in which “road noise,” due to dragging the tool over rough and hard borehole wall in the carbonates, caused unreliable measurements of apparent velocity. Reprocessing (see “Explanatory Notes” chapter, this volume) may not improve the data, and residual problems are likely (Fig. 20).

The NGT is one of the few logging tools that can provide useful formation data through drill pipe. Through-pipe spectral gamma-ray logs were obtained for the upper portion of Hole 867B. For the through-pipe interval, the total gamma-ray and uranium signals are above the noise level of the tool, but all values for thorium and potassium are near or below its resolving power. For the open-hole interval, replicate spectral gamma-ray logs exhibit modest agreement for uranium and almost no agreement for both potassium and thorium. The latter two elements are present in such low quantities at Hole 867B that their logs fluctuate about zero, and the total gamma-ray signal is attributable almost entirely to uranium (Fig. 20).

Each log was adjusted in depth, by correlating the gamma-ray logs between runs, to correct for differences in the stretch of the logging cable. All logs were then corrected to the base of the drill pipe by subtracting the depth from the rig floor to the seafloor (1363.2 m). These depths should be accurate within ± 2 m.

Velocity, Resistivity, and Density Relationships

Velocity, resistivity, and density correlate well throughout the entire logged interval at Hole 867B (Fig. 20). Furthermore, these three logs are correlated moderately well with the gamma-ray log (SGR in Fig. 20); gamma-ray maxima correspond to velocity, resistivity, and density minima. The uranium enrichment pattern is real, but the thorium content of these rocks is so low that small variations in the thorium log may actually be a uranium-based artifact of the spectral gamma-ray inversion. Although uncalibrated as to absolute porosity, all five porosity-sensitive logs (Fig. 20) exhibit strong interlog correlations and, consequently, are considered to be good indicators of variations in relative porosity in Hole 867B.

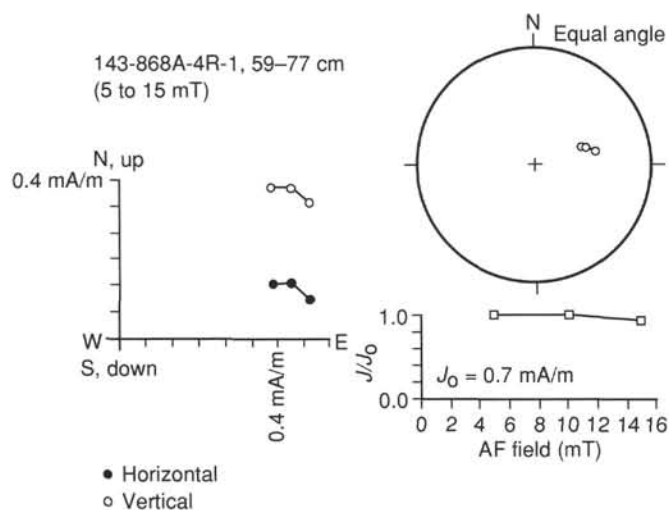


Figure 13. Discrete sample (143-868A-4R-1, 59–77 cm) shows typical behavior of segments of reddish limestone from Hole 868A. Equal angle stereonet plot (upper right) of magnetization vector end points at 5, 10, and 15 mT AF demagnetization steps. Plot (lower right) showing normalized intensity remaining at various AF demagnetization steps. Orthogonal vector plot (left) of vector end points during AF demagnetization.

The changes in velocity and density with depth generally show no evidence of a simple compaction profile, suggesting that mechanical compaction over the 59-m logged interval is minor in comparison to original depositional texture and diagenesis in controlling porosity at this site. This pattern is similar to that observed at Site 865. The logged interval exhibits a complex character, apparently with substantial changes involving varying degrees of sorting and cementation, in addition to more substantial facies changes.

Log-based Units

Two log units can be defined, based on the combined geophysical and natural gamma-ray log responses:

Logging Unit 1, from just below the pipe to 23.6 mbsf, has resistivity values of 10 to 100 ohm-m. The lithologic Subunit IIA/IIB contact (at 18.3 mbsf) is just barely in the open hole, and its presence in the velocity and resistivity logs (Fig. 20) is doubtful. The boundary between logging Units 1 and 2 is sharply defined in all logs; the discrepancy between this boundary and the lithologic Subunit IIA/IIB boundary may have been caused by poor recovery in this area. This unit is much higher in resistivity, density, and velocity than the underlying unit, implying much lower porosity. Analysis of the processed FMS images will be required to interpret the style of porosity variations at a vertical resolution one to two orders of magnitude higher than is obtainable from the logs of Figure 20.

The sharp decrease in resistivity at the boundary between logging Units 1 and 2 indicates a substantial change in the relationship between the pore morphology and the flow of electric current through pore fluids. A plausible explanation is that the moldic porosity contains vugs that are poorly connected; the porosity may not change, but the electrical resistance measured is controlled to a significant degree by small channels that may connect relatively large vugs. The lower unit thus may have cyclic moldic porosity within layers of varying cementation, where velocity is controlled by high bulk porosity and resistivity varies, depending on the connectivity of the vuggy pore spaces.

Logging Unit 2, from 23.6 mbsf to the end of the logging run at 74 mbsf, has a resistivity that increases gradually downhole from about 1 to 900 ohm-m, but is punctuated by intervals having higher values, indicating layers of variable cementation. This is consistent with the heterogeneity identified for lithologic Subunit IIB from the core analysis (see "Lithostratigraphy" section, this chapter), although the limited core recovery does not allow for matching of individual beds between core and log. A thin, high-resistivity layer occurs at

Table 2. Concentrations of total, inorganic, and organic carbon and of total nitrogen and sulfur in sediments from Holes 867B and 868A.

Core, section, interval (cm)	Depth (mbsf)	Sample type ^a	TC (%)	IC (%)	TOC (%)	CaCO ₃ (%)	N (%)	S (%)	TOC/N	TOC/S
Hole 867B										
1R-2, 15–16	1.51	CARB	12.14	12.00	0.14	100.0	0.01	0.00	14.0	
1R-2, 29–30	1.65	IWSC	12.07	11.99	0.08	99.9	0.00	0.00		
2R-1, 87–89	8.97	CARB	11.97	11.82	0.15	98.5	0.00	0.00		
4R-1, 9–10	18.19	CARB	11.90	11.87	0.03	98.9	0.02	0.00	1.0	
4R-1, 79–80	18.89	CARB	12.18	11.99	0.19	99.9	0.01	0.00	19.0	
4R-2, 61–62	20.21	CARB	12.04	11.85	0.19	98.7	0.00	0.00		
4R-4, 49–50	23.09	CARB	12.01	11.90	0.11	99.1	0.00	0.00		
5R-1, 31–32	24.81	CARB	11.91	11.90	0.01	99.1	0.00	0.00		
6R-1, 28–29	34.18	CARB	11.98	11.97	0.01	99.7	0.00	0.03		0.3
8R-1, 96–97	53.46	CARB	12.04	11.94	0.10	99.5	0.00	0.00		
9R-1, 20–21	62.00	CARB	11.81	11.40	0.41	95.0	0.01	0.00	41.0	
10R-1, 54–56	66.94	CARB	12.17	11.91	0.26	99.2	0.00	0.00		
11R-1, 23–24	68.63	CARB	11.92	11.88	0.04	99.0	0.00	0.00		
12R-1, 98–99	72.38	CARB	12.19	11.90	0.29	99.1	0.00	0.00		
12R-2, 132–133	74.13	CARB	12.08	11.88	0.20	99.0	0.01	0.00	20.0	
13R-1, 61–62	75.91	CARB	12.18	11.96	0.22	99.6	0.02	0.00	11.0	
Hole 868A										
1R-1, 116–117	1.16	PP		11.99		99.9				
1R-2, 32–34	1.82	PP		11.96		99.6				
2R-1, 49–50	8.49	CARB	12.13	11.95	0.18	99.5	0.01	0.03	18.0	6.0
3R-1, 102–104	12.12	PP		11.97		99.7				
3R-2, 48–51	12.90	PP		11.97		99.7				
4R-1, 31–33	13.41	PP		12.00		100.0				
4R-1, 87–88	13.97	CARB	12.06	11.97	0.09	99.7	0.02	0.01	4.0	9.0
4R-2, 44–46	14.90	PP		12.00		100.0				
4R-2, 55–56	15.01	PP		12.00		100.0				
5R-1, 70–71	17.90	CARB	12.08	11.98	0.10	99.8	0.01	0.00	10.0	

^a Sample type: CARB = carbonate; IWSC = interstitial-water squeeze cake; PP = physical property.

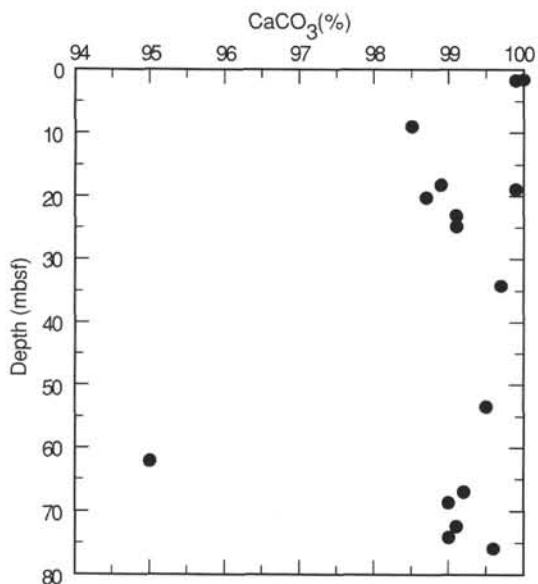


Figure 14. Depth distribution of calcium carbonate concentration in Hole 867B.

62 mbsf. This is a single layer, unlike those in Hole 865A, where many thin high-resistivity layers were intercalated with layers having lower values. The lower resistivity zones coincide with lower velocities and large hole diameters, suggesting weaker unlithified material that has been preferentially removed during the drilling process.

Logging Unit 2 cementation must be variable with depth, as seen in the highly variable velocities, resistivities, and densities (Fig. 20). The unit appears to be composed of a single "upward-coarsening" packet, but the term may be inappropriate for these observed diagenetic porosity variations than for primary sedimentary variations. Gross characteristics are typical for grainstones grading to wackestones and mudstones. The underlying mudstones-wackestones are consistently lower in porosity (i.e., higher in resistivity and velocity), with a baseline shift occurring at 53.4 mbsf. Velocity, density, and resistivity values are also high; this pattern implies that the rigidity and intergranular cementation increase downhole, substantially reducing porosity.

The most distinctive gamma-log response within logging Unit 2 is a sudden decrease to very low values (uranium content) at 62.0 mbsf, increasing to ambient uranium concentrations by 67.3 mbsf. Its cause is uncertain, but the spike of high resistivity indicates that it is probably a diagenetic horizon.

Conclusions

Lithologic Unit I (0–0.29 mbsf) was not logged. The limestones of lithologic Subunit IIA (0.29–18.3 mbsf) are phosphatized and display multiple generations of internal sediments. The downward percolation of the phosphatization is confirmed both by sedimentary structure in the cores and by the apparent leaching of uranium from the lower portion of lithologic Subunit IIA to 22 mbsf, as indicated in the natural gamma-ray log. The "beach deposits" of Subunit IIA, corresponding to the highly resistive log Unit 1, have (keystone) vugular porosity with voids up to 2 to cm in size that gradually increase in abundance, while decreasing in size with greater depth. Lithologic Subunit IIB (18.3–76.9 mbsf) consists of lagoonal sediments with moldic porosity, becoming very fine-grained and grossly vugular downsection. This is reflected in the highly variable resistivity and porosity logs. One explanation of this pattern is that log Unit 2

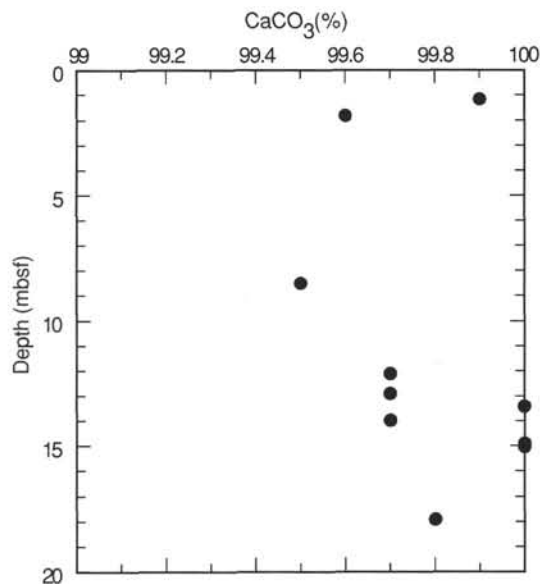


Figure 15. Depth distribution of calcium carbonate concentration in Hole 868A.

was exposed and underwent extensive subaerial(?) diagenetic dissolution and cementation/recrystallization. Subsequent submergence allowed for resumption of sedimentation to form logging Unit 1. The succeeding sediments are much lower in porosity (and less recrystallized?) than underlying logging Unit 2 sediments. This exposure and submergence may have been caused by eustatic changes in sea level or by local uplift and subsidence.

REFERENCES*

- Coogan, A.H., 1977. Early and Middle Cretaceous Hippuritacea (Rudists) of the Gulf Coast. In Bebout, D.G., and Loucks, R.G. (Eds.), *Cretaceous Carbonates of Texas and Mexico: Applications to Subsurface Exploration*. Rep. Invest.—Univ. Tex. Austin, Bur. Econ. Geol., 89:32–70.
- Esteban, M., and Klappa, C.F., 1983. Subaerial exposure environment. In Scholle, P.A., Bebout, D.G., and Moore, C.H. (Eds.), *Carbonate Depositional Environments*. AAPG Mem., 33:1–54.
- Flügel, E., and Steiger, T., 1981. An Upper Jurassic sponge-algal buildup from the northern Frankenalb, West Germany. In Toomey, D.F. (Ed.), *European Fossil Reef Models*. Spec. Publ.—Soc. Econ. Paleontol. Mineral., 30:371–397.
- Hallock, P., and Schlager, W., 1986. Nutrient excess and the demise of coral reefs and carbonate platforms. *Palaios*, 1:389–398.
- Palmer, R., 1928. The rudistids of southern Mexico. *Occas. Pap. Calif. Acad. Sci.*, 14:1–137.
- Shipboard Scientific Party, 1981. Site 463: western Mid-Pacific Mountains. In Thiede, J., Vallier, T.L., et al., *Init. Repts. DSDP*, 62: Washington (U.S. Govt. Printing Office), 33–156.
- Skelton, P., 1982. Aptian and Barremian rudist bivalves of the New World: some old world similarities. *Cretaceous Res.*, 3:145–153
- van Waasbergen, R.J., and Winterer, E.L., in press. Summit geomorphology of Western Pacific guyots. In Pringle, M.S., Sager, W.W., Sliter, W.V., and Stein, S. (Eds.), *The Mesozoic Pacific*. Am. Geophys. Union, Geophys. Monogr. Ser.

* Abbreviations for names of organizations and publication titles in ODP reference lists follow the style given in *Chemical Abstracts Service Source Index* (published by American Chemical Society).

Ms 143IR-108

NOTE: For all sites drilled, core-description forms ("barrel sheets") and core photographs have been reproduced on coated paper and can be found in Section 3, beginning on page 381. Forms containing smear-slide data can be found in Section 4, beginning on page 691. Conventional and geochemical-log, FMS, and dipmeter data can be found in CD-ROM form (back pocket).

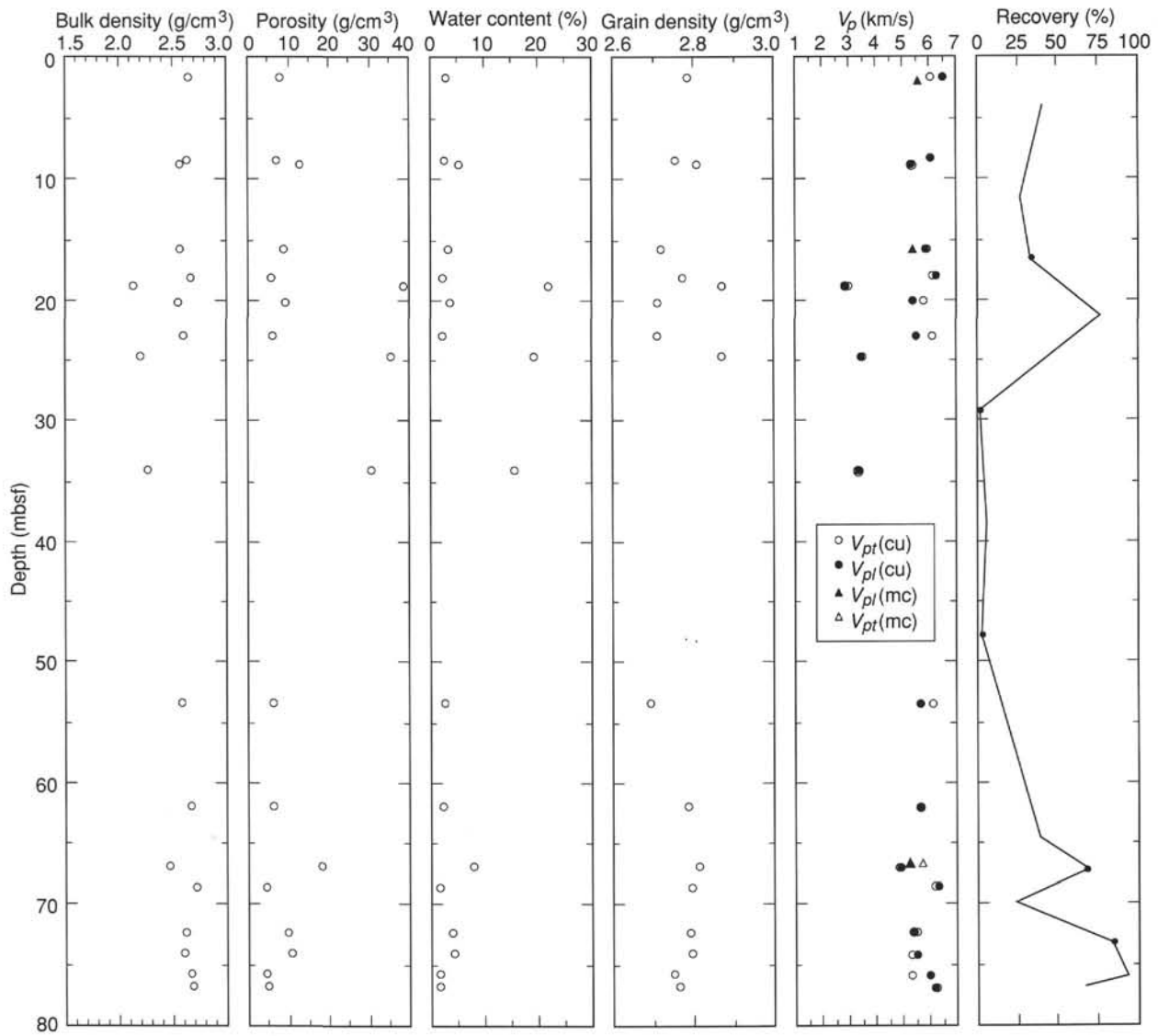


Figure 16. Index properties, sonic velocity, and recovery data for Hole 867B. V_{pt} is transverse; V_{pl} is longitudinal (parallel to core axis); bracketed letters in legend indicate measurements from cubes (cu) or measurements from minicores (mc).

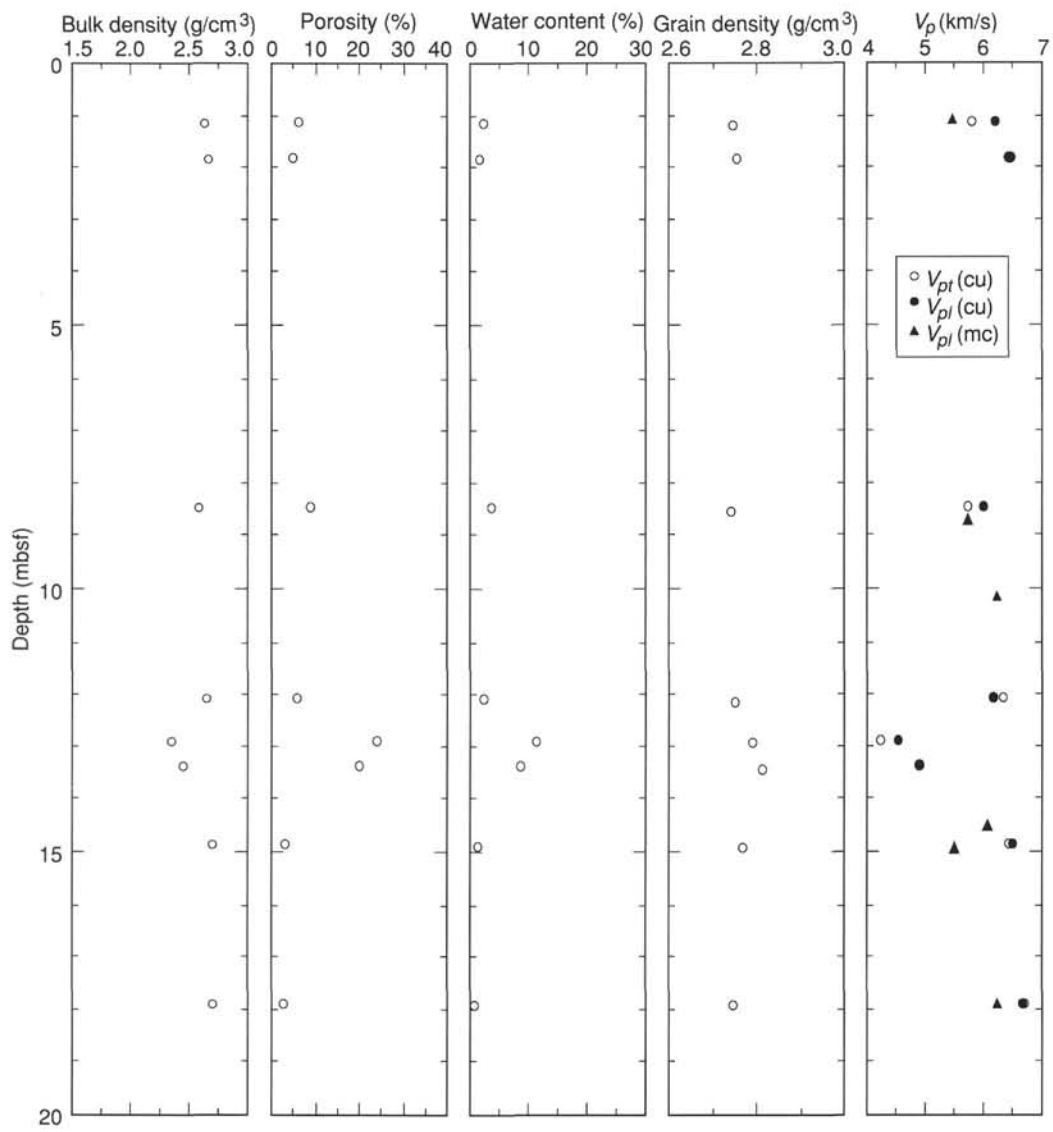


Figure 17. Index properties and sonic velocity data for Hole 868A. V_{pt} is transverse; V_{pl} is longitudinal (parallel to core axis); bracketed letters in legend indicate measurements from cubes (cu) or measurements from minicores (mc).

Table 3. Index properties, Holes 867B and 868A.

Core, section interval (cm)	Depth (mbsf)	Water content (%)	Bulk density (g/cm ³)	Grain density (g/cm ³)	Porosity (%)
143-867B-					
1R-2, 14-17	1.67	3.09	2.65	2.79	7.94
2R-1, 35-37	8.46	2.81	2.63	2.76	7.19
2R-1, 73-75	8.84	5.28	2.58	2.81	12.92
3R-1, 80-82	15.91	3.57	2.57	2.72	8.87
4R-1, 7-10	18.19	2.33	2.67	2.78	6.08
4R-1, 78-80	18.89	22.04	2.15	2.87	38.77
4R-2, 60-62	20.21	3.78	2.56	2.71	9.30
4R-4, 48-50	23.09	2.52	2.60	2.71	6.40
5R-1, 29-31	24.80	19.37	2.20	2.87	35.76
6R-1, 26-28	34.17	15.65	2.27	2.83	30.70
8R-1, 95-97	53.46	2.62	2.58	2.70	6.59
9R-1, 19-23	62.02	2.38	2.68	2.79	6.21
10R-1, 53-56	66.95	8.09	2.48	2.81	18.54
11R-1, 21-23	68.62	1.79	2.71	2.80	4.77
12R-1, 96-98	72.37	3.97	2.62	2.79	9.98
12R-2, 130-132	74.12	4.39	2.60	2.80	10.95
13R-1, 59-61	75.90	1.79	2.67	2.75	4.70
14B-1, 4-6	76.85	1.84	2.68	2.77	4.85
143-868A-					
1R-1, 116-117	1.17	2.45	2.64	2.75	6.31
1R-2, 32-34	1.83	1.87	2.67	2.76	4.91
2R-1, 48-51	8.50	3.70	2.58	2.74	9.22
3R-1, 102-104	12.13	2.34	2.65	2.75	6.07
3R-2, 48-51	12.92	11.45	2.36	2.79	24.21
4R-1, 31-33	13.42	8.85	2.45	2.81	19.93
4R-2, 44-46	14.91	1.27	2.71	2.77	3.39
5R-1, 72-74	17.93	1.08	2.70	2.75	2.88

Table 4. Sonic velocity, anisotropy, and bulk density, Holes 867B and 868A.

Core, section, interval (cm)	Depth (mbsf)	$V_p(\text{cu})$ (km/s)	$V_{pt}(\text{cu})$ (km/s)	$V_{pm}(\text{cu})$ (km/s)	$V_{pt}(\text{mc})$ (km/s)	Anisotropy (cu) (%)	Anisotropy (mc) (%)	Bulk density (g/cm ³)
143-867B-								
1R-2, 14-17	1.67	6.052	6.519				-7.699	2.65
1R-2, 47-49	1.98				5.589			
2R-1, 35-37	8.46	6.046	6.045				-0.151	2.63
2R-1, 73-75	8.84	5.327	5.344				0.186	2.58
3R-1, 80-82	15.91	5.913	5.900				0.777	2.57
3R-1, 82-85	15.94				5.405			
4R-1, 7-10	18.19	6.139	6.274				-3.351	2.67
4R-1, 78-80	18.89	3.038	2.879				-6.383	2.15
4R-2, 60-62	20.21	5.843	5.441				-9.376	2.56
4R-4, 48-50	23.09	6.138	5.543				-2.407	2.60
5R-1, 29-31	24.80	3.515	3.507				-3.947	2.20
6R-1, 26-28	34.17	3.364	3.444				-4.202	2.27
8R-1, 95-97	53.46	6.119	5.660				-8.178	2.58
9R-1, 19-23	62.02	5.656	5.646				0.907	2.67
10R-1, 27-31	66.69				5.309			
10R-1, 32-36	66.74			5.761		8.166		
10R-1, 53-56	66.95	4.881	4.913				-1.696	2.48
11R-1, 21-23	68.62	6.209	6.317				-8.260	2.71
12R-1, 96-98	72.37	5.546	5.384				-6.300	2.62
12R-2, 130-132	74.12	5.321	5.521				-7.720	2.60
13R-1, 59-61	75.90	5.348	6.023				6.946	2.67
14R-1, 4-6	76.85	6.299	6.232				1.069	2.68
143-868A-								
1R-1, 109-111	1.10				5.474			
1R-1, 116-117	1.17	5.808	6.203				-6.579	2.64
1R-2, 32-34	1.83	6.428	6.489				-0.936	2.67
2R-1, 48-51	8.50	5.746	6.014				-4.567	2.58
2R-1, 72-75	8.74				5.732			
2R-2, 69-71	10.20				6.235			
3R-1, 102-104	12.13	6.346	6.183				2.597	2.65
3R-2, 48-51	12.92	4.259	4.533				-6.238	2.36
4R-1, 31-33	13.42	4.898	4.908				-0.206	2.45
4R-2, 8-13	14.56				6.093			
4R-2, 44-46	14.91	6.431	6.498				-1.044	2.71
4R-2, 52-56	15.00				5.500			
5R-1, 72-74	17.93	6.724	6.662				0.920	2.70
5R-1, 75-77	17.96				6.230			

Note: Measurements are labeled for direction and sample-shape: $V_{pu}(\text{cu})$ is from an unoriented cube; $V_{pt}(\text{cu})$ is transverse (horizontal) from a cube; $V_{pm}(\text{cu})$ is longitudinal (parallel core axis) from a cube; $V_{pt}(\text{mc})$ is transverse from a minicore; $V_{pm}(\text{mc})$ is longitudinal from a minicore.

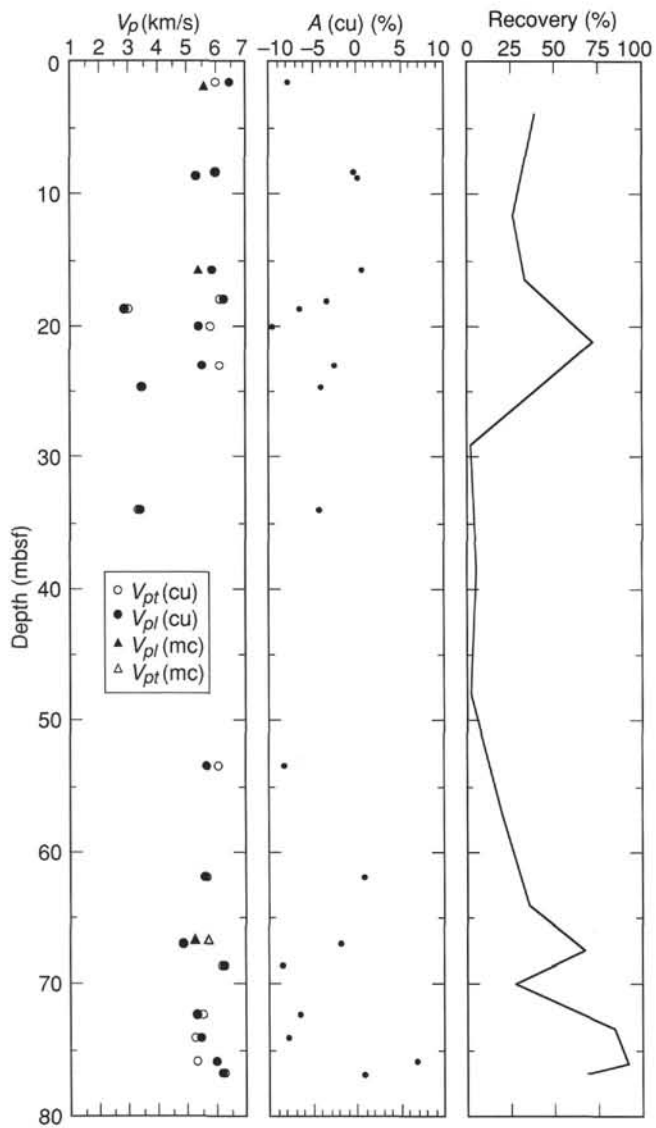


Figure 18. Plot of sonic velocity, anisotropy, and recovery for Hole 867B. V_{pt} is transverse; V_{pl} is longitudinal (parallel to core axis); bracketed letters in legend indicate measurements from cubes (cu) or measurements from minicores (mc).

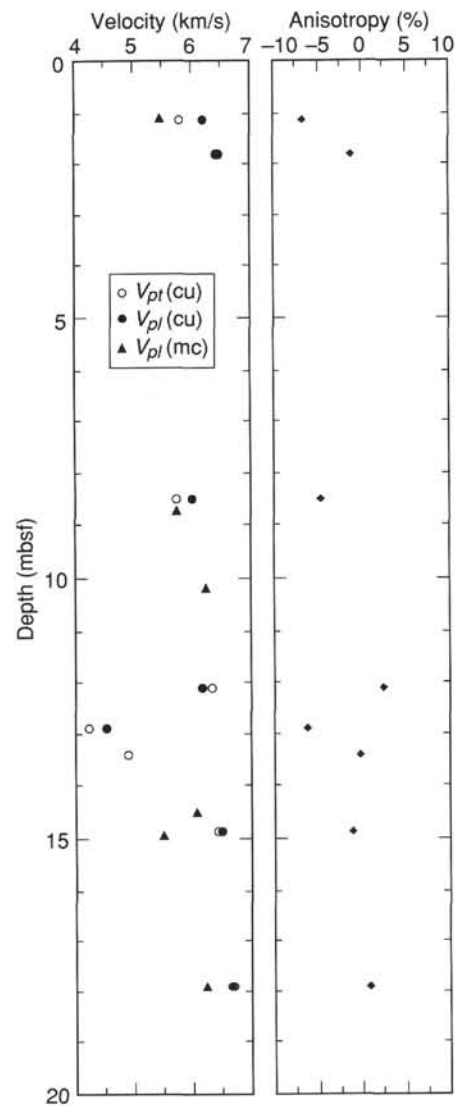


Figure 19. Plot of sonic velocity and anisotropy for Hole 868A. V_{pt} is transverse; V_{pl} is longitudinal (parallel to core axis); bracketed letters in legend indicate measurements from cubes (cu) or measurements from minicores (mc).

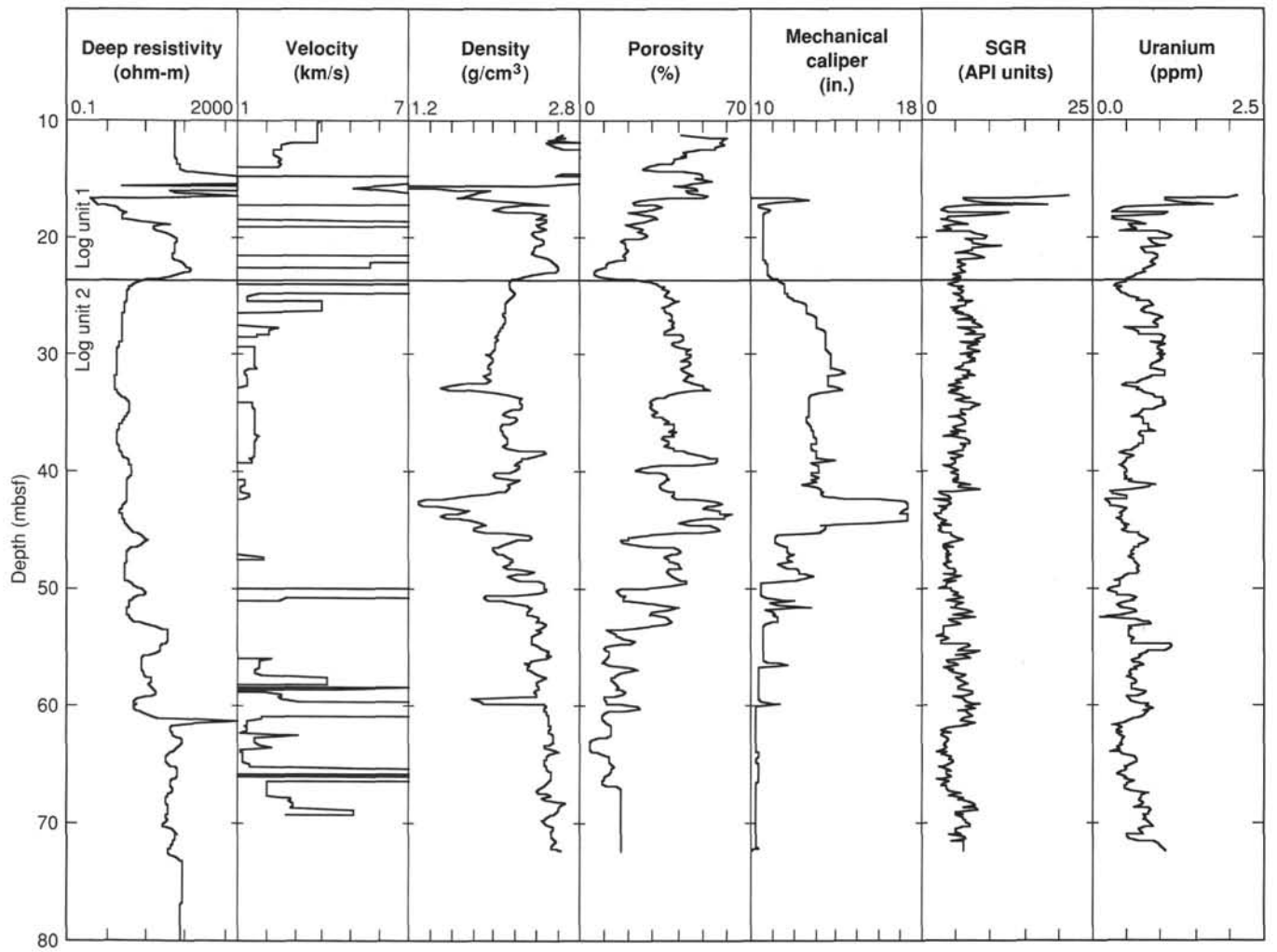
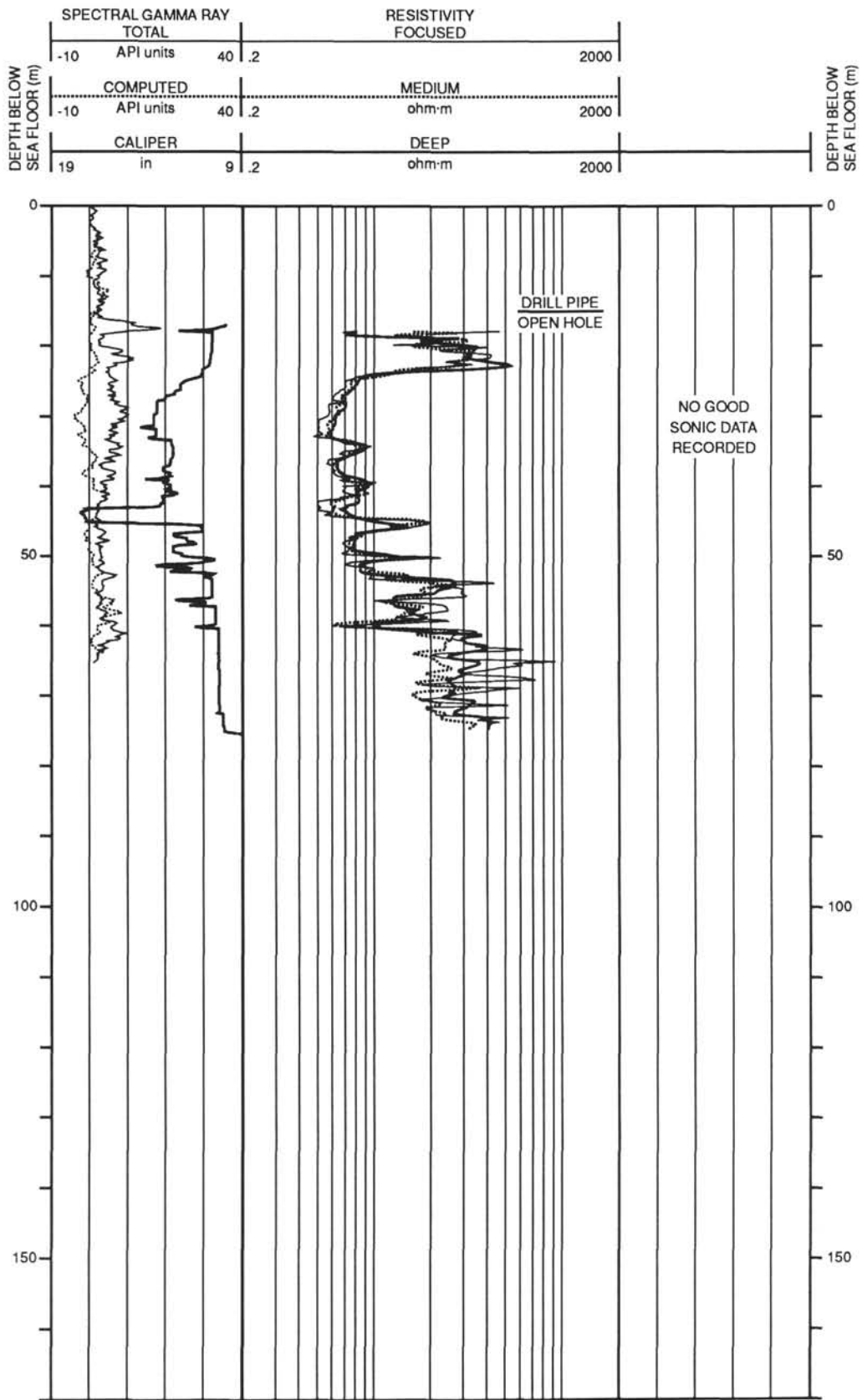


Figure 20. Geophysical and gamma-ray logs from Hole 867B.

Hole 867B: Resistivity-Natural Gamma Ray Log Summary



Hole 867B: Density-Porosity-Natural Gamma Ray Log Summary

